

ORIGINAL ARTICLE

EVI-1 interacts with histone methyltransferases SUV39H1 and G9a for transcriptional repression and bone marrow immortalization

S Goyama^{1,2}, E Nitta¹, T Yoshino¹, S Kako¹, N Watanabe-Okochi¹, M Shimabe¹, Y Imai¹, K Takahashi² and M Kurokawa¹

¹Department of Hematology and Oncology, Graduate School of Medicine, University of Tokyo, Bunkyo-ku, Tokyo, Japan and

²Department of Transfusion Medicine, Graduate School of Medicine, University of Tokyo, Bunkyo-ku, Tokyo, Japan

The ecotropic viral integration site-1 (EVI-1) is a nuclear transcription factor and has an essential function in the proliferation/maintenance of haematopoietic stem cells. Aberrant expression of EVI-1 has been frequently found in myeloid leukaemia as well as in several solid tumours, and is associated with a poor patient survival. It was recently shown that EVI-1 associates with two different histone methyltransferases (HMTs), SUV39H1 and G9a. However, the functional roles of these HMTs in EVI-1-mediated leukemogenesis remain unclear. In this study, we showed that EVI-1 physically interacts with SUV39H1 and G9a, but not with Set9. Immunofluorescence analysis revealed that EVI-1 colocalizes with these HMTs in nuclei. We also found that the catalytically inactive form of SUV39H1 abrogates the transcriptional repression mediated by EVI-1, suggesting that SUV39H1 is actively involved in EVI-1-mediated transcriptional repression. Furthermore, RNAi-based knockdown of SUV39H1 or G9a in EVI-1-expressing progenitors significantly reduced their colony-forming activity. In contrast, knockdown of these HMTs did not impair bone marrow immortalization by E2A/HLF. These results indicate that EVI-1 forms higher-order complexes with HMTs, and this association has a role in the transcription repression and bone marrow immortalization. Targeting these HMTs may be of therapeutic benefit in the treatment for EVI-1-related haematological malignancies.

Leukemia (2010) 24, 81–88; doi:10.1038/leu.2009.202;
published online 24 September 2009

Keywords: EVI-1; SUV39H1; G9a; epigenetics

Introduction

The ecotropic viral integration site-1 (*Evi-1*) gene was first identified as a common locus of retroviral integration in murine leukaemia models.^{1,2} In humans, *EVI-1* is located on chromosome 3q26, and rearrangements on chromosome 3q26 often activate EVI-1 expression in myelodysplastic syndrome (MDS) and acute myeloid leukaemia. Importantly, high EVI-1 expression is an independent negative prognostic indicator of survival in acute myeloid leukaemia, irrespective of the presence of 3q26 rearrangements.^{3,4} EVI-1 possesses diverse functions as an oncoprotein. EVI-1 antagonizes growth-inhibitory effects of transforming growth factor- β (TGF- β);⁵ protects cells from stress-induced cell death by inhibiting c-Jun N-terminal kinase;⁶ increases the expression of endogenous c-Jun and c-fos, resulting in the activation of AP-1.⁷ Mouse models in which *Evi-1* is retrovirally expressed in haematopoietic cells showed that activation of *Evi-1* leads to myeloid dysplasia,⁸ whereas the

development of full-blown leukaemia requires additional genetic events.^{9,10} Furthermore, recent gene targeting studies in mice revealed that *Evi-1* has an essential function in the proliferation/maintenance of haematopoietic stem cells.^{11,12}

EVI-1 contains DNA-binding zinc finger motifs and belongs to the positive regulatory (PR) domain family of transcription factors, which are characterized by the presence of multiple zinc fingers and a PR domain at the N-terminus.¹³ The PR domain is a subclass of the evolutionarily conserved SET domain, which has been linked to chromatin-mediated gene regulation and histone methylation. There are two major alternative forms generated from *EVI-1* gene, EVI-1 (PR-absent form) and MDS1-EVI-1 (PR-containing form, also called EVI-1c) (Figure 1a). Although related, functional differences between EVI-1 and MDS1-EVI-1 have been documented.^{14,15} In addition to its DNA-binding activity, EVI-1 has the potential to recruit diverse proteins, such as Smad3, HDACs and CtBP,^{5,16–18} thus generating complexes for transcriptional regulation.

Methylation of specific histone residues has an essential regulatory function in gene transcription. Specifically, methylation of histoneH3 lysine 9 (H3K9) is associated with gene silencing. After the initial identification of SUV39H1 as a H3K9-specific histone methyltransferase (HMT),¹⁹ at least three other HMTs, G9a, GLP and SETDB1, have been recognized as HMTs for H3K9 in mammals.²⁰ Very recently, two independent groups reported that EVI-1 physically interacts with the H3K9 HMTs, SUV39H1 and G9a.^{21,22} However, functional roles of these HMTs in EVI-1-mediated leukemogenesis remain unclear.

In this study, we showed that EVI-1 interacts and colocalizes with SUV39H1 and G9a. Remarkably, RNAi-based knockdown of these HMTs in *Evi-1*-expressing progenitors significantly reduced their colony-forming activity, suggesting that these HMTs could be therapeutic targets in poor prognosis leukaemia with aberrant EVI-1 expression.

Materials and methods

DNA constructs

The plasmid pME18S-Flag-EVI-1, pME18S-Flag-MDS1-EVI-1, pMXs-neo-E2A/HLF (a gift from T Inaba) have been described earlier.^{12,14} The pCMV-Myc-SUV39H1 and pEGFPC1-G9a were gifts from M Tachibana and Y Shinkai. SUV39H1-H324K was created by PCR mutagenesis to change amino acid 324 from histidine to lysine. The pCDNA3.1HA-G9a and pCDNA3.1HA-G9a-NH903/904LE were gifts from K Wright. The pCDNA3.1-Flag-Set9 was a gift from D Reinberg. Mouse *Evi-1* cDNA was obtained using the mRNA prepared from para-aortic splanchnopleura (P-Sp) region of the embryo, and inserted into the pGCDNsam-eGFP retroviral vector (a gift from H Nakauchi and M Onodera).

Correspondence: Professor M Kurokawa, Department of Hematology and Oncology, Graduate School of Medicine, University of Tokyo, 7-3-1 Hongo, Bunkyo-ku, Tokyo 113-8655, Japan.

E-mail: kurokawa-tky@umin.ac.jp

Received 8 April 2009; revised 11 August 2009; accepted 24 August 2009; published online 24 September 2009

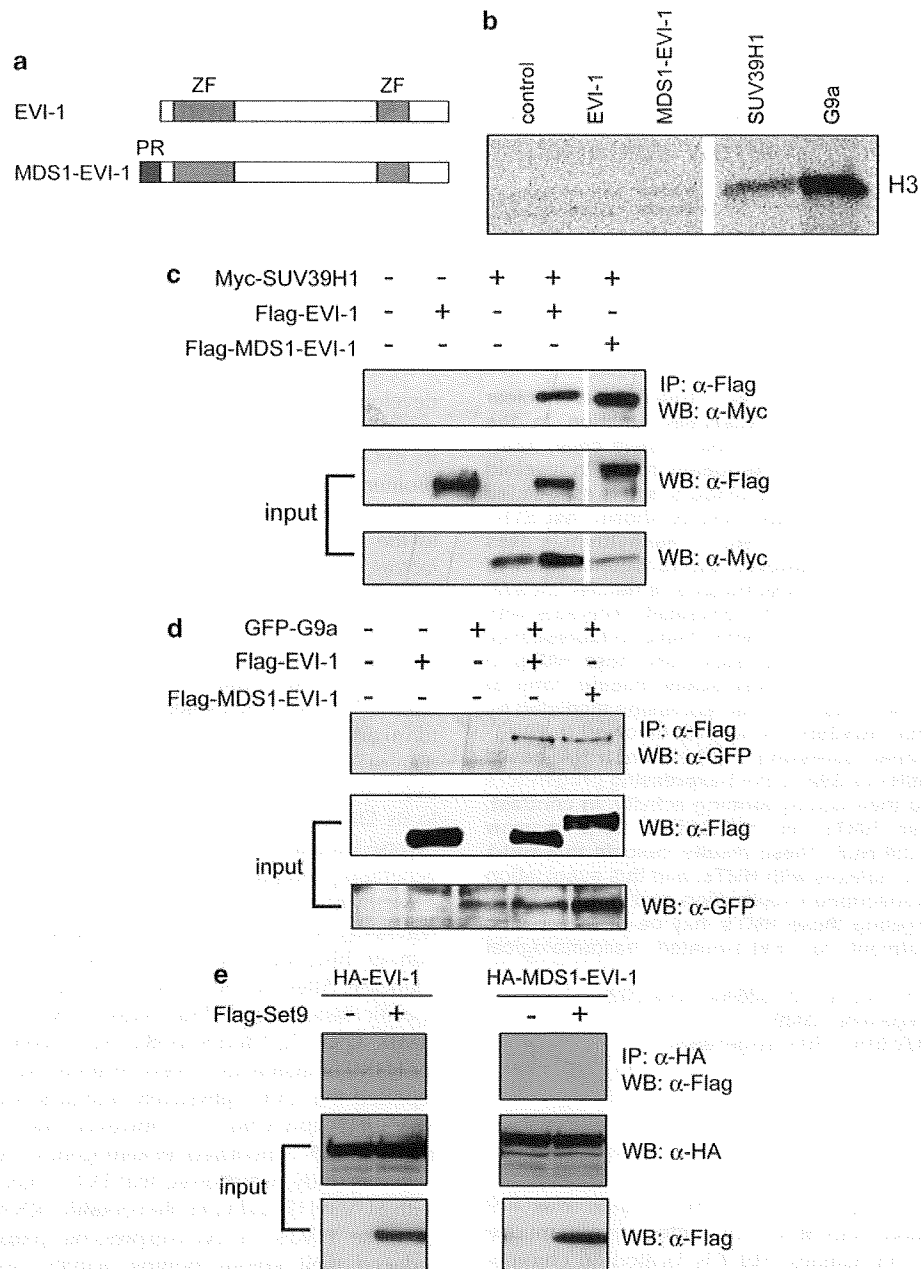


Figure 1 EVI-1 interacts with histone methyltransferases SUV39H1 and G9a, but not with Set9. (a) Schematic representation of EVI-1 isoforms. ZF, zinc finger domain; PR, PR domain. (b) Histone methyltransferase assay with FLAG-EVI-1 and Flag-MDS1-EVI-1. Lysates from cells transfected with EVI-1 or MDS1-EVI-1 were immunoprecipitated with anti-Flag antibody and analysed for specific histone H3 methylation activity by autoradiography, but neither EVI-1 nor MDS1-EVI-1 methylated histone H3. Myc-SUV39H1 and HA-G9a were purified with anti-Myc or HA antibodies and used as positive controls. (c) The 293T cells were transfected with Flag-EVI-1 (lanes 2 and 4), Flag-MDS1-EVI-1 (lane 5), and Myc-SUV39H1 (lanes 3–5). Whole-cell extracts were immunoprecipitated with anti-Flag antibody. Flag-EVI-1-bound Myc-SUV39H1 was detected by western blotting by means of anti-Myc (top). Expression of Flag-EVI-1 and Myc-SUV39H1 is monitored with anti-Flag (middle) and anti-Myc (bottom), respectively. (d) The 293T cells were transfected with Flag-EVI-1 (lanes 2 and 4), Flag-MDS1-EVI-1 (lane 5), and GFP-G9a (lanes 3–5). Whole-cell extracts were immunoprecipitated with anti-Flag antibody. Flag-EVI-1-bound GFP-G9a was detected by western blotting by means of anti-GFP (top). Expression of Flag-EVI-1 and GFP-G9a is monitored with anti-Flag (middle) and anti-GFP (bottom), respectively. (e) The 293T cells were transfected with HA-EVI-1 (left panel), HA-MDS1-EVI-1 (right panel) and Flag-Set9 (lane 2 of both panels). Whole-cell extracts were immunoprecipitated with anti-HA antibody. HA-EVI-1-bound Flag-Set9 was detected by western blotting by means of anti-Flag (top). Expression of HA-EVI-1 and Flag-Set9 is monitored with anti-HA (middle) and anti-Flag (bottom), respectively.

HMT assay

Flag-EVI-1, Myc-SUV39HA or HA-G9a was immunoprecipitated with anti-Flag, anti-Myc and anti-HA antibodies, respectively. The immunoprecipitates were incubated for 1 h at 37 °C in 50 µl of MAB buffer (50 mM Tris, pH 8.5, 20 mM KCl, 10 mM

MgCl₂, 10 mM β-mercaptoethanol, 250 mM sucrose) containing 2 µg of histone 3 (Roche, Indianapolis, IN, USA) as the substrate and S-adenosyl-[methyl-¹⁴C]-l-methionine as the methyl donor. Reactions were stopped by boiling the samples in sodium dodecyl sulphate loading buffer, and then the proteins were separated by

15% sodium dodecyl sulphate-polyacrylamide gel electrophoresis. Gels were dried and quantification of methyl-¹⁴C was performed using a BAS-2000 imaging analyzer (Fuji Film).

Immunoprecipitation and western blotting

The 293T cells were transfected by the calcium phosphate method. The cells were cultured 48 h after transfection and were lysed in the TNE buffer.¹⁴ For immunoprecipitation, cell lysates were incubated with the anti-Flag M2 monoclonal antibody (F3165, Sigma, St Louis, MO, USA) for 3 h at 4 °C. Then, the samples were incubated with protein-G-Sepharose (Amersham Pharmacia Biotech, Piscataway, NJ, USA) for 1 h at 4 °C. The precipitates were washed five times with the TNE buffer, subjected to sodium dodecyl sulphate-polyacrylamide gel electrophoresis, and analysed by western blotting. Western blotting was performed with anti-Flag M2-Peroxidase (A8592, Sigma), anti-Myc (2276, Cell Signaling Technology, Beverly, MA, USA), anti-HA-Peroxidase (12CA5, Roche), anti-GFP antibody (G1544, Sigma), anti-EVI-1 (C50E12, Cell Signaling Technology), anti-SUV39H1 (MG44, upstate) or anti-G9a antibody (C6H3, Cell Signaling Technology). Proteins were visualized by the enhanced chemiluminescence system (Amersham Pharmacia Biotech).

Immunofluorescence microscopy

For colocalization studies, COS7 cells were transfected with Myc-SUV39H1 or GFP-G9a together with Flag-EVI-1 using the

FuGENE transfection reagent (Roche). After 48 h, cells were fixed in 3.7% formaldehyde and permealized with 0.1% Triton X-100. Samples were blocked with 1% bovine serum albumin for 40 min, incubated with mouse anti-Myc-FITC (F2047, Sigma) or rabbit anti-Flag antibody (F7425, Sigma) for 2 h, washed, and then incubated with the Alexa Fluor 555 conjugated goat anti-rabbit antibody. For evaluation of endogenous H3K9 methylation status, MEF cells were incubated with rabbit anti-dimethyl H3K9 (29698, Upstate) or rabbit anti-trimethyl H3K9 antibody (31855, Upstate), followed by labelling with Alexa Fluor 488 conjugated anti-rabbit antibody. Nuclear staining was performed using TOPRO3 (Invitrogen, Carlsbad, CA, USA). Cells were analysed by the confocal laser scanning microscopy (Leica TCS SL).

Luciferase reporter assay

For analysis of luciferase activities, 293T cells were seeded in 12-well culture plates at a density of 1×10^5 per well. At 12 h after seeding, the cells were transfected with 500 ng of p3TP-Lux, 100 ng of pME-EVI-1, and increasing amounts (100 or 200 ng) of either pcDNA3-SUV39H1, pcDNA3-SUV39H1-H324K, pcDNA3-G9a or pcDNA3-G9a-NH903/904LE using Lipofectamin 2000 (Invitrogen). The cells were harvested 48 h after transfection and assayed for the luciferase activity by means of the luciferase assay system (Promega, Madison, WI, USA) and a luminometer (Lumat, LB 9700, Berthold, Bad Wildbad, Germany). Transfection efficiency was evaluated by cotransfecting 10 ng of a reporter CMV-βgalactosidase plasmid.

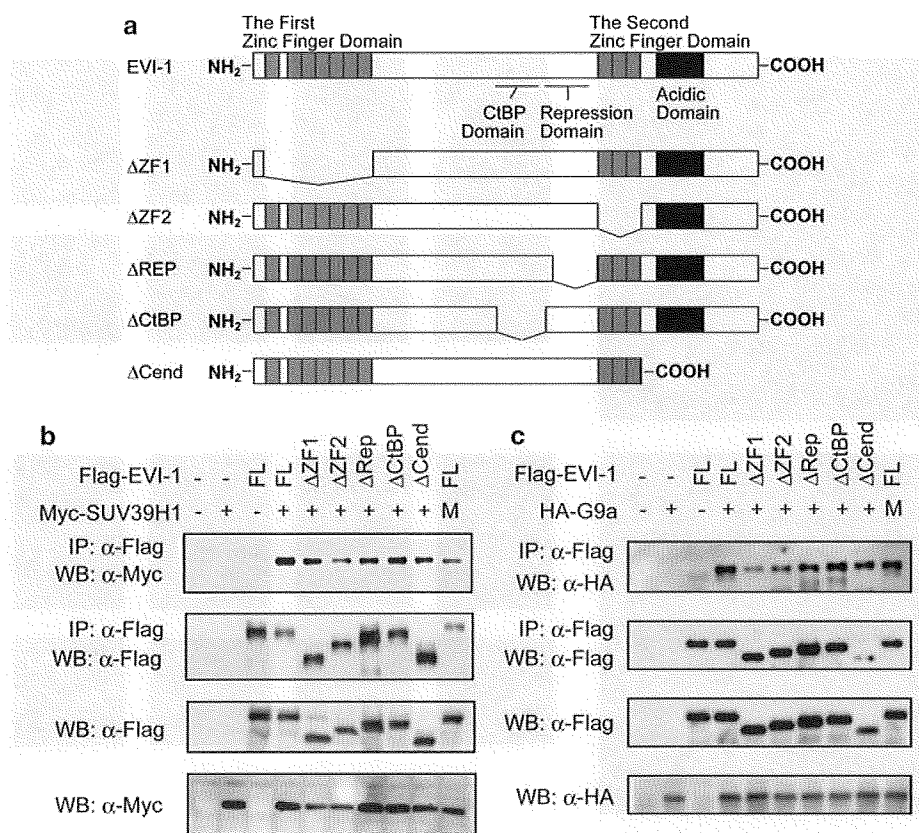


Figure 2 Domain contribution of EVI-1 for interaction with SUV39H1 and G9a. (a) Schematic presentation of the functional domains of EVI-1 and structures of the deletion mutants. (b) Association between Flag-EVI-1 or its deletion mutants and Myc-SUV39H1 or its mutant. M, a mutant carrying an inactivating point mutation within the HMT domain of SUV39H1 (SUV39H1-H324K). (c) Association between Flag-EVI-1 or its deletion mutants and HA-G9a or its mutant. M, a mutant carrying an inactivating point mutation within the HMT domain of G9a (G9a-NH903/904LE).

Retrovirus transduction and colony-replating assay

Plat-E packaging cells²³ were transiently transfected with 3 μ g of retrovirus vectors, mixed with 9 μ l of FuGENE 6 (Roche) for retrovirus production. Colony-replating assay was performed as described earlier.²⁴ Colony-forming cells from the third to fifth round of plating were subsequently infected with retrovirus encoding either Suv39H1-small hairpin RNA (shRNA), G9a-shRNA or control-shRNA, and the cells were replated at 1×10^5 per plate in M3434 in the presence of 1 μ g/ml puromycin. Puromycin-resistant colonies were then replated at 5×10^3 per plate.

RNA interference

We designed retrovirus vectors (RNAi-Ready pSIREN-RetroQ Vector, Clontech, Palo Alto, CA, USA) encoding an shRNA directed against murine Suv39h1 or G9a. As a control, we used an shRNA vector without hairpin oligonucleotides. Reduced expression of Suv39H1 or G9a in Evi-1- or E2A/HLF-immortalized cells was confirmed by performing quantitative PCR with Universal ProbeLibrary Reference Gene Assays (Roche). Target sequences for shRNAs and primer sequences for quantitative PCR are shown in Supplementary Table 1.

Statistical analysis

Statistical significance of differences between parameters was assessed using Welch's *t*-test.

Results

EVI-1 associates with SUV39H1 and G9a in mammalian cells

As PR domain is homologous to the catalytic SET domains of HMTs, we initially assessed whether MDS1-EVI-1 (PR-containing form) is able to transfer methyl groups onto histones. We purified recombinant full-length EVI-1 and MDS1-EVI-1 from 293T cell extracts by immunopurification and analysed them by an *in vitro* HMT assay with histone H3 as a substrate. However, the immunoprecipitated EVI-1 protein (both EVI-1 and MDS1-EVI-1) had no methyltransferase activity (Figure 1b), indicating that MDS1-EVI-1 itself is not a HMT. We then investigated whether EVI-1 can associate with H3K9-specific HMTs, SUV39H1 and G9a in mammalian cells. We introduced Flag-tagged EVI-1 or MDS1-EVI-1 in the absence or presence of Myc-SUV39H1 into 293T cells. Cell lysates were subjected to immunoprecipitation with anti-Flag, followed by immunoblotting with anti-Myc. We observed that Myc-SUV39H1 was coprecipitated with both Flag-EVI-1 and Flag-MDS1-EVI-1 (Figure 1c). Using the same assay, we also found that GFP-G9a could be detected in immunoprecipitates of both Flag-EVI-1 and Flag-MDS1-EVI-1 (Figure 1d). In contrast, Flag-SET9 did not show any interaction with HA-EVI-1 (Figure 1e). Thus, both isoforms of EVI-1 are able to form a complex with two H3K9 methyltransferases, SUV39H1 and G9a.

We next mapped the region of EVI-1 that is necessary for interaction with the HMTs using EVI-1 deletion mutants that lack various functional domains (Figure 2a).²⁵ The first zinc

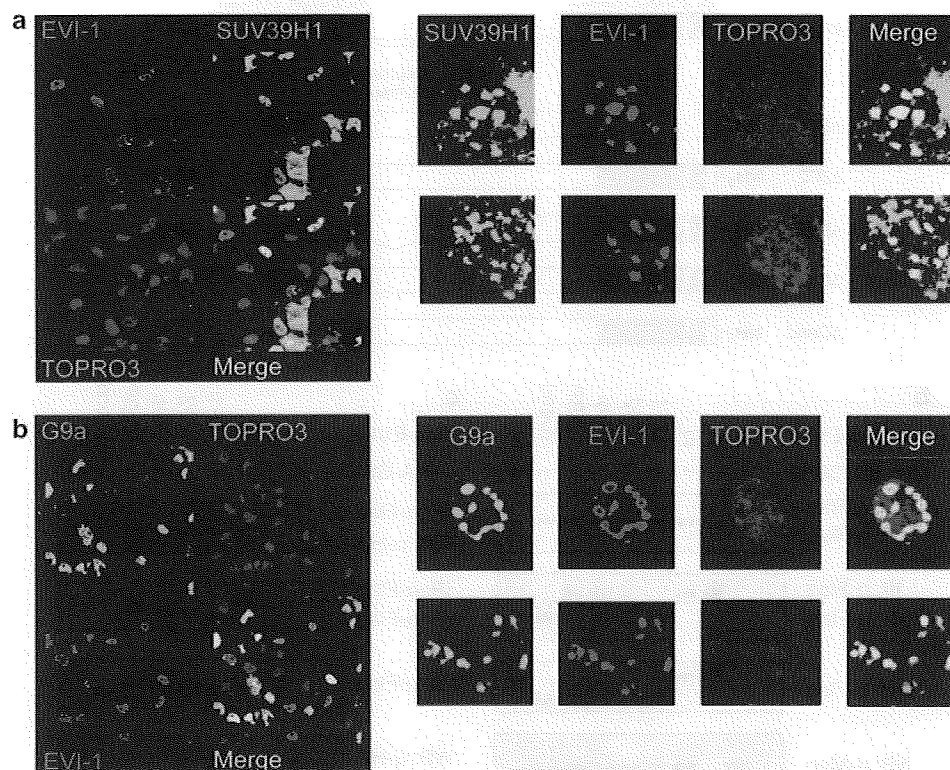


Figure 3 EVI-1 colocalizes with histone methyltransferases SUV39H1 and G9a in the nucleus. (a) COS7 cells were cotransfected with Myc-SUV39H1 and Flag-EVI-1 and stained with anti-Myc-FITC (green) and anti-Flag antibodies followed by secondary Alexa 555 (red) staining, together with TOPRO3 nuclei staining (blue). Merged images revealed the partial association of both proteins in speckled structures of the nucleus. (b) COS7 cells were cotransfected with GFP-G9a (green) and Flag-EVI-1 and stained with anti-Flag followed by secondary Alexa Fluor 555 (red) staining, together with TOPRO3 nuclei staining (blue). Merged images revealed nearly complete association of both proteins in speckled structures of the nucleus.

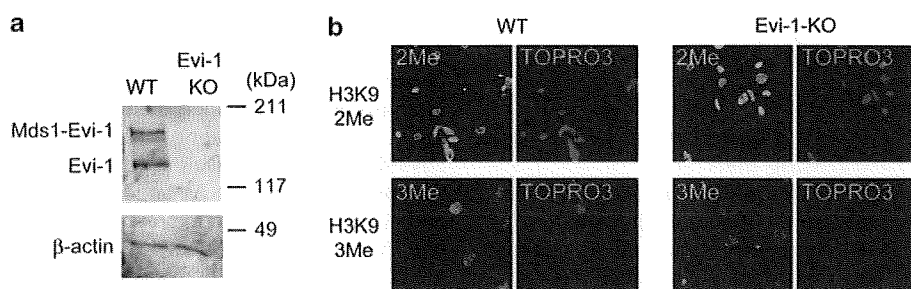


Figure 4 EVI-1 deficiency does not affect global methylation status in MEF cells. (a) Expression of Evi-1 and β -actin protein in wild-type and Evi-1^{-/-} MEF cells. (b) Wild-type (left panel) and Evi-1^{-/-} (right panel) MEFs were stained for H3K9-Me2 (upper panel) or H3K9-Me3 (lower panel), followed by secondary Alexa 488 (green), together with TOPRO3 nuclei staining (blue). H3K9-2Me and 3Me were broadly detected in nuclei of MEF cells, and Evi-1^{-/-} cells showed no remarkable change on the overall methylation level.

finger domain (ZF1) is a DNA-binding domain and is essential for interaction with several proteins, including Smad3 and c-Jun N-terminal kinase.^{5,6} The second zinc finger domain (ZF2) is another DNA-binding domain and is essential for AP-1 activation.⁷ The repression domain is required for the efficient repression of TGF- β signalling.⁵ The region containing CtBP-binding-motif-like sequences is responsible for the interaction with CtBP1.¹⁶ In addition, EVI-1 contains a highly acidic domain at the C-terminus, which is required for EVI-1-mediated P-Sp haematopoiesis.²⁶ In contrast to the earlier reports, which showed that EVI-1 interacts with SUV39H1 through ZF1,^{21,22} all of these deletion mutants associate with both SUV39H1 and G9a almost as efficiently as full-length EVI-1 (Figure 2b and c). These results indicate that the interactions between EVI-1 and HMTs are mediated through a relatively wide stretch of multiple regions, at least in 293T cells.

EVI-1 colocalizes with SUV39H1 and G9a in the nucleus

Next, we examined whether EVI-1 and the HMTs could colocalize in cells using immunofluorescence analysis with COS7 cells. Consistent with earlier reports,²⁷ EVI-1 shows a nuclear diffused localization pattern in the majority of cells, and sometimes shows speckled nuclear distribution (Figure 3a and b, left). When both Flag-tagged EVI-1 and Myc-tagged SUV39H1 were cotransfected into COS7 cells, EVI-1 and SUV39H1 formed speckles that partially overlap (yellow colour) in nuclei, confirming the colocalization between two proteins *in vivo* (Figure 3a, right). The possibility of cross-talk between the channels or cross-reactivity of the antibodies was ruled out (Supplementary Figure 1). The same assay also revealed nearly complete colocalization of EVI-1 and G9a in cells transfected with both constructs (Figure 3b, right). Thus, EVI-1 and the HMTs (SUV39H1 and G9a) colocalize within the nucleus in mammalian cells.

EVI-1 is not essential for the global methylation of H3K9

It has been shown that SUV39H1 is required for H3K9 trimethylation (H3K9-3Me) and G9a promotes H3K9 dimethylation (H3K9-2Me).²⁸ Therefore, we then examined the effect of Evi-1 deletion on the overall levels of di- and tri-methylation of H3K9 in wild-type and Evi-1^{-/-} MEF cells. The absence of Evi-1 protein in Evi-1^{-/-} MEF cells was confirmed by western blotting (Figure 4a). As shown in Figure 4b, H3K9-2Me and 3Me were broadly detected in nuclei of MEF cells, and Evi-1^{-/-} cells showed no remarkable change on overall methylation levels.

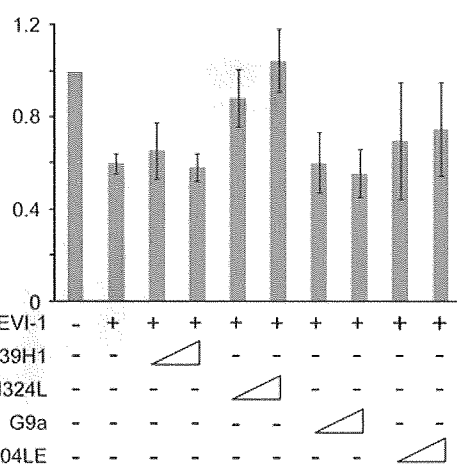


Figure 5 Transcriptional repression by EVI-1 requires catalytically active SUV39H1. The 293T cells were cotransfected with p3TP-Lux and expression vectors for EVI-1, and different concentrations of the SUV39H1, SUV39H1-H324K, G9a and G9a-NH903/904LE, as indicated. All luciferase assays were performed in triplicates in two independent experiments. Values and error bars depict the mean and the s.d., respectively.

Thus, EVI-1 deficiency does not cause significant reduction of H3K9 methylation level in MEF cells.

Transcriptional repression by EVI-1 requires catalytically active SUV39H1

We next investigated whether SUV39H1 and G9a are actively involved in EVI-1-mediated transcriptional repression. We transfected 293T cells with the reporter plasmid p3TP-Lux, a synthetic TGF- β -responsive reporter that contains the promoter region of the plasminogen activator inhibitor 1 (PAI-1). As shown earlier, cotransfection of EVI-1 resulted in repression of the reporter activity. Interestingly, increasing amounts of SUV39H1-H324K, a construct carrying an inactivating point mutation within the HMT domain of SUV39H1, completely abrogated the transcriptional repression mediated by EVI-1 (Figure 5). As H324K is still able to associate with EVI-1 in immunoprecipitation studies (Figure 2b), it is thought to act as a dominant-negative mutant by competing with endogenous SUV39H1. In contrast, both G9a and G9a-NH903/904LE, a construct carrying inactivating mutations within the HMT domain of G9a, did not affect the reporter activity (Figure 5).

These results suggest that SUV39H1 is more important for Evi-1-mediated transcriptional repression in this context.

Both SUV39H1 and G9a are required for efficient propagation of Evi-1-expressing cells

We then evaluated a role for HMTs in Evi-1-induced leukemogenesis. Bone marrow cells from 5-fluorouracil-treated mice were transduced with Evi-1, and were subjected to colony-replating assay (Figure 6a). Consistent with earlier reports,²⁹ primary bone marrow progenitors transduced with Evi-1, but not empty vector, formed colonies in methylcellulose that can be replated through at least seven rounds of culture (data not

shown). Wright-Giemsa-stained cytopsin preparations of the cells constituting these Evi-1-transduced colonies showed blastic morphology with myeloid dysplasia (Figure 6b). After establishment of sustained clonogenic activity after more than three rounds of replating, the cells were transduced with Suv39h1-shRNA, G9a-shRNA or control-shRNA. We designed two independent shRNAs targeting murine Suv39H1 or G9a, and confirmed reduced expression of these HMTs by quantitative PCR in Evi-1-transduced cells and by western blotting in NIH3T3 cells (Figure 6c; Supplementary Figure 2). Although the colony-forming activity vary among different cultures (Supplementary Table 2), knockdown of Suv39h1 or G9a in Evi-1-transduced progenitors showed a clear tendency to reduce

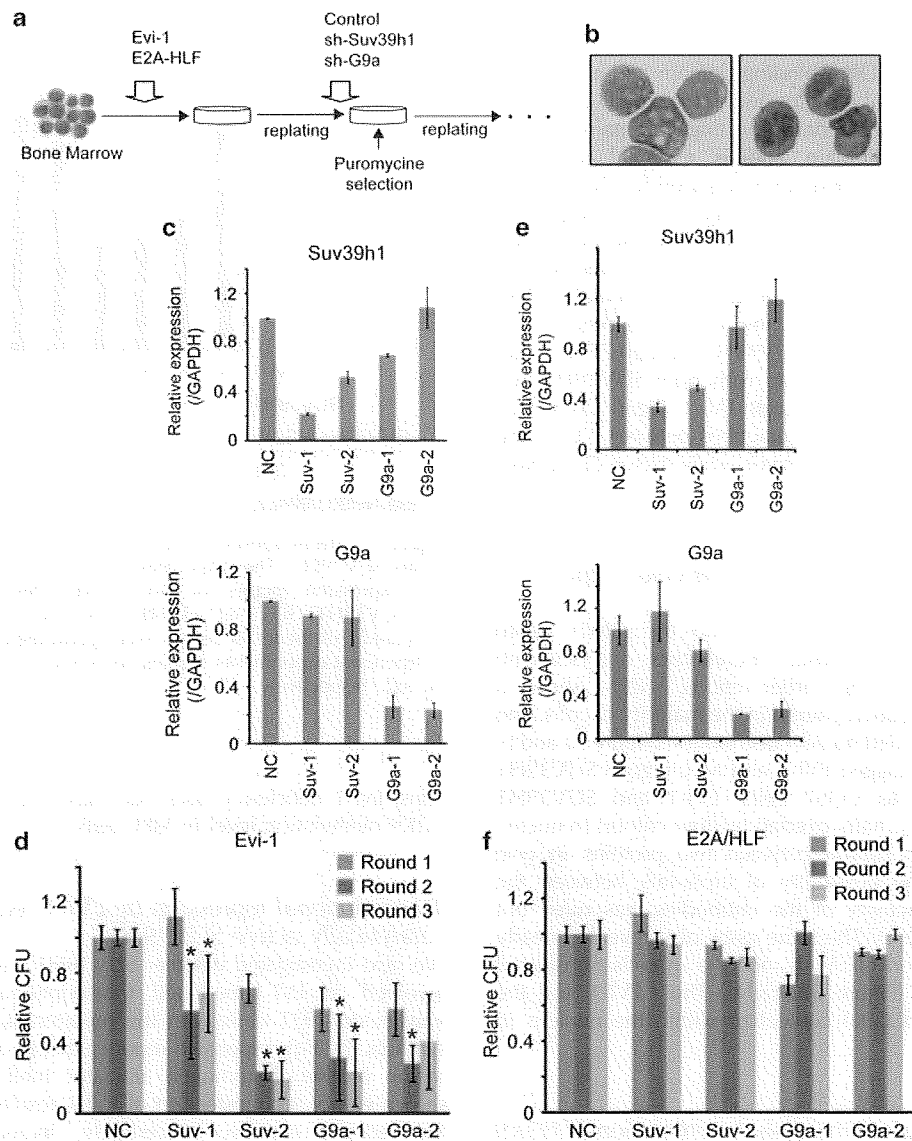


Figure 6 Effects of SUV39H1 or G9a knockdown on Evi-1-induced bone marrow immortalization. (a) Schematic representation of the following experiments. BM progenitors were transduced with Evi-1 or E2A/HLF oncogenes. Colony-forming cells from the third to fifth round of *in vitro* plating were subsequently transduced with Suv39h1-shRNA, G9a-shRNA or control-shRNA. Clonogenic activity was then assessed in the further round of replating in the presence of puromycin. (b) Giemsa-stained cells constituting colonies generated by Evi-1. Blasts (left panel) and the cells with Pseudo-Pelger-Huet anomaly (right panel) were shown. (c, e) Relative expression of Suv39h1 or G9a in Evi-1-immortalized cells (c) or E2A/HLF-immortalized cells (e) transduced with various shRNAs. Values are normalized to GAPDH. Means from two independent experiments are depicted with s.d. NC, negative control; Suv-1, 2, shRNAs for Suv39h1; G9a-1, 2, shRNAs for G9a. (d, f) Colony counts from the replating cultures of Evi-1- or E2A/HLF-immortalized cells after shRNA transduction. The bar graph shows the relative number of colonies generated by HMT-downregulated cells compared with control cells. Means from five (Evi-1) or three (E2A/HLF) independent experiments are depicted with s.d., each in duplicate. Statistical analysis was performed on Round2 and Round3 colony numbers. * $P < 0.01$, relative to controls.

the colony numbers (Figure 6d; Supplementary Figure 3A; Supplementary Table 2). In addition, the HMT-knockdown cells exhibited a tendency to differentiate towards a granulocytic lineage in some experiments (Supplementary Figure 3B). We then assessed a role for the HMTs in bone marrow immortalization by E2A/HLF, a chimeric gene generated in t(17;19) that is also known to immortalize murine bone marrow cells.³⁰ We used E2A/HLF as a control because the contribution of Evi-1 to colony-forming ability of E2A/HLF-transduced cells is relatively small.¹² Despite the efficient downregulation of Suv39h1 and G9a (Figure 6e), the HMT-knockdown cells showed equivalent colony-forming activity to that of control E2A/HLF-transduced cells (Figure 6f; Supplementary Table 2). These results indicate that both Suv39h1 and G9a are specifically required for Evi-1-mediated bone marrow immortalization.

Discussion

Understanding mechanisms underlying EVI-1-mediated leukemogenesis is essential to develop new therapy for leukaemias with high EVI-1 expression, which are often predictive of poor clinical outcome. Very recently, it was shown that EVI-1 physically interacts with H3K9 HMTs,^{21,22} suggesting that EVI-1 regulates transcription by recruiting these HMTs. Here, we extended these analyses and found that the HMTs are important for colony-replating ability of Evi-1.

The PR domain is a subclass of SET domains most closely related to the known HMTs. However, we found that MDS1-EVI-1 (PR-containing form) showed no HMT activity. It was shown earlier that PRDI-BF1 (Blimp-1), another member of PR gene family, exhibits HMT activity by recruiting G9a regardless of its PR domain.³¹ Similarly, as we and others have shown, EVI-1 interacts with two HMTs, SUV39H1 and G9a. Therefore, it is likely that EVI-1 is involved in histone modification by recruiting other proteins, not through its PR domain.

Earlier reports showed that wild-type SUV39H1 enhances the repressive potential of Gal4-EVI-1 on the activity of a promoter-containing GAL4 sites, whereas the effect is not observed when the catalytically inactive mutant (SUV39H1-H324K) was used.^{21,22} In contrast to these reports, we found that SUV39H1-H324K acts in a dominant-negative manner to abrogate EVI-1-mediated repression of p3TP-Lux reporter activity, whereas wild-type SUV39H1 has little effect on the repression by EVI-1. This discrepancy is probably because of the different cell types and/or promoters used for the assays. Thus, SUV39H1 is actively involved in EVI-1-mediated transcription but its effects are strictly dependent on the context. Although we did not observe significant changes in the EVI-1-mediated p3TP reporter repression by G9a or its catalytically inactive mutant (G9a-NH903/904LE), the possible requirement of G9a for EVI-1-mediated transcriptional regulation should be assessed in different experimental settings. Furthermore, because genes downregulated by EVI-1 have not been identified thus far, identification of repressive target genes of EVI-1 is an important future challenge.

Downregulation of Suv39h1 or G9a in Evi-1-transduced cells significantly inhibited their colony-forming activity. It may indicate the importance of these HMTs for generation of leukaemia-initiating cells by Evi-1. Alternatively, these HMTs may support efficient propagation of Evi-1-expressing leukaemic cells. To clarify a precise role of Evi-1/HMT complex in leukemogenesis, further *in vivo* studies are warranted. In contrast to Evi-1-induced immortalization, both Suv39h1 and G9a are dispensable for bone marrow immortalization by

E2A/HLF. Although we have shown that complete loss of Evi-1 slightly reduced colony-forming ability of E2A/HLF, the effect of Evi-1 deletion in E2A/HLF-immortalized cells is relatively small than that in MLL-immortalized cells.¹² It therefore seems likely that the Evi-1/HMT interaction is not a major mediator for oncogenic activity of E2A/HLF.

Recently, several inhibitors targeting SUV39H1 and G9a have been identified.^{32,33} Furthermore, we have shown that a HDAC inhibitor, trichostatin A, alleviates Evi-1-mediated repression of TGF- β signalling.¹⁶ Therefore, combined epigenetic therapy with the HMT and the HDAC inhibitors may exert synergistic activity against EVI-1-expressing leukaemic cells, and it also needs to be evaluated in the future.

In summary, we showed that EVI-1 interacts and colocalizes with SUV39H1 and G9a. The interaction contributes, at least in part, to the transcriptional repression and bone marrow immortalization by EVI-1. Although further studies are required to address the mechanistic links between histone methylation and EVI-1-mediated leukemogenesis, our results indicate that targeting these HMTs could be of therapeutic benefit in the treatment for EVI-1-related haematological malignancies.

Conflict of interest

The authors declare no conflict of interest.

Acknowledgements

We thank T Kitamura for Plat-E packaging cells, H Nakauchi and M Onodera for pGCDNsam-eGFP retroviral vector, T Inaba, M Tachibana, Y Shinkai, K Wright and D Reinberg for cDNAs (see Materials and methods), Y Shimamura for expert technical assistance, and KYOWA KIRIN for cytokines. This work was supported in part by a Grant-in-Aid for Scientific Research from the Japan Society for the Promotion of Science, and by Health and Labour Sciences Research grants from the Ministry of Health, Labour and Welfare.

References

- Morishita K, Parker DS, Mucenski ML, Jenkins NA, Copeland NG, Ihle JN. Retroviral activation of a novel gene encoding a zinc finger protein in IL-3-dependent myeloid leukemia cell lines. *Cell* 1988; **54**: 831–840.
- Mucenski ML, Taylor BA, Ihle JN, Hartley JW, Morse III HC, Jenkins NA *et al*. Identification of a common ecotropic viral integration site, Evi-1, in the DNA of AKXD murine myeloid tumors. *Mol Cell Biol* 1988; **8**: 301–308.
- Valk PJ, Verhaak RG, Beijen MA, Erpelinck CA, Barjesteh van Waalwijk van Doorn-Khosrovani S, Boer JM *et al*. Prognostically useful gene-expression profiles in acute myeloid leukemia. *N Engl J Med* 2004; **350**: 1617–1628.
- Lugthart S, van Drunen E, van Norden Y, van Hoven A, Erpelinck CA, Valk PJ *et al*. High EVI1 levels predict adverse outcome in acute myeloid leukemia: prevalence of EVI1 overexpression and chromosome 3q26 abnormalities underestimated. *Blood* 2008; **111**: 4329–4337.
- Kurokawa M, Mitani K, Irie K, Matsuyama T, Takahashi T, Chiba S *et al*. The oncoprotein Evi-1 represses TGF-beta signalling by inhibiting Smad3. *Nature* 1998; **394**: 92–96.
- Kurokawa M, Mitani K, Yamagata T, Takahashi T, Izutsu K, Ogawa S *et al*. The evi-1 oncoprotein inhibits c-Jun N-terminal kinase and prevents stress-induced cell death. *EMBO J* 2000; **19**: 2958–2968.
- Tanaka T, Nishida J, Mitani K, Ogawa S, Yazaki Y, Hirai H. Evi-1 raises AP-1 activity and stimulates c-fos promoter transactivation with dependence on the second zinc finger domain. *J Biol Chem* 1994; **269**: 24020–24026.

- 8 Buonamici S, Li D, Chi Y, Zhao R, Wang X, Brace L *et al*. EVI1 induces myelodysplastic syndrome in mice. *J Clin Invest* 2004; **114**: 713–719.
- 9 Jin G, Yamazaki Y, Takuwa M, Takahara T, Kaneko K, Kuwata T *et al*. Trib1 and Evi1 cooperate with Hoxa and Meis1 in myeloid leukemogenesis. *Blood* 2007; **109**: 3998–4005.
- 10 Watanabe-Okochi N, Kitaura J, Ono R, Harada H, Harada Y, Komeno Y *et al*. AML1 mutations induced MDS and MDS/AML in a mouse BMT model. *Blood* 2008; **111**: 4297–4308.
- 11 Yuasa H, Oike Y, Iwama A, Nishikata I, Sugiyama D, Perkins A *et al*. Oncogenic transcription factor Evi1 regulates hematopoietic stem cell proliferation through GATA-2 expression. *EMBO J* 2005; **24**: 1976–1987.
- 12 Goyama S, Yamamoto G, Shimabe M, Sato T, Ichikawa M, Ogawa S *et al*. Evi-1 is a critical regulator for hematopoietic stem cells and transformed leukemic cells. *Cell Stem Cell* 2008; **3**: 207–220.
- 13 Fears S, Mathieu C, Zeleznik-Le N, Huang S, Rowley JD, Nucifora G. Intergenic splicing of MDS1 and EVI1 occurs in normal tissues as well as in myeloid leukemia and produces a new member of the PR domain family. *Proc Natl Acad Sci USA* 1996; **93**: 1642–1647.
- 14 Nitta E, Izutsu K, Yamaguchi Y, Imai Y, Ogawa S, Chiba S *et al*. Oligomerization of Evi-1 regulated by the PR domain contributes to recruitment of corepressor CtBP. *Oncogene* 2005; **24**: 6165–6173.
- 15 Sood R, Talwar-Trikha A, Chakrabarti SR, Nucifora G. MDS1/EVI1 enhances TGF-beta1 signaling and strengthens its growth-inhibitory effect but the leukemia-associated fusion protein AML1/MDS1/EVI1, product of the t(3;21), abrogates growth-inhibition in response to TGF-beta1. *Leukemia* 1999; **13**: 348–357.
- 16 Izutsu K, Kurokawa M, Imai Y, Maki K, Mitani K, Hirai H. The corepressor CtBP interacts with Evi-1 to repress transforming growth factor beta signaling. *Blood* 2001; **97**: 2815–2822.
- 17 Palmer S, Brouillet JP, Kilbey A, Fulton R, Walker M, Crossley M *et al*. Evi-1 transforming and repressor activities are mediated by CtBP co-repressor proteins. *J Biol Chem* 2001; **276**: 25834–25840.
- 18 Vinatzer U, Taplick J, Seiser C, Fonatsch C, Wieser R. The leukaemia-associated transcription factors EVI-1 and MDS1/EVI1 repress transcription and interact with histone deacetylase. *Br J Haematol* 2001; **114**: 566–573.
- 19 Rea S, Eisenhaber F, O'Carroll D, Strahl BD, Sun ZW, Schmid M *et al*. Regulation of chromatin structure by site-specific histone H3 methyltransferases. *Nature* 2000; **406**: 593–599.
- 20 Tachibana M, Sugimoto K, Fukushima T, Shinkai Y. Set domain-containing protein, G9a, is a novel lysine-preferring mammalian histone methyltransferase with hyperactivity and specific selectivity to lysines 9 and 27 of histone H3. *J Biol Chem* 2001; **276**: 25309–25317.
- 21 Cattaneo F, Nucifora G. EVI1 recruits the histone methyltransferase SUV39H1 for transcription repression. *J Cell Biochem* 2008; **105**: 344–352.
- 22 Spensberger D, Delwel R. A novel interaction between the proto-oncogene Evi1 and histone methyltransferases, SUV39H1 and G9a. *FEBS Lett* 2008; **582**: 2761–2767.
- 23 Kitamura T, Koshino Y, Shibata F, Oki T, Nakajima H, Nosaka T *et al*. Retrovirus-mediated gene transfer and expression cloning: powerful tools in functional genomics. *Exp Hematol* 2003; **31**: 1007–1014.
- 24 Takeshita M, Ichikawa M, Nitta E, Goyama S, Asai T, Ogawa S *et al*. AML1-Evi-1 specifically transforms hematopoietic stem cells through fusion of the entire Evi-1 sequence to AML1. *Leukemia* 2008; **22**: 1241–1249.
- 25 Goyama S, Kurokawa M. Pathogenetic significance of ecotropic viral integration site-1 in hematological malignancies. *Cancer Sci* 2009; **100**: 990–995.
- 26 Sato T, Goyama S, Nitta E, Takeshita M, Yoshimi M, Nakagawa M *et al*. Evi-1 promotes para-aortic splanchnopleural hematopoiesis through up-regulation of GATA-2 and repression of TGF- β signaling. *Cancer Sci* 2008; **99**: 1407–1413.
- 27 Chakraborty S, Senyuk V, Sitailo S, Chi Y, Nucifora G. Interaction of EVI1 with cAMP-responsive element-binding protein-binding protein (CBP) and p300/CBP-associated factor (P/CAF) results in reversible acetylation of EVI1 and in co-localization in nuclear speckles. *J Biol Chem* 2001; **276**: 44936–44943.
- 28 Peters AH, Kubicek S, Mechtler K, O'Sullivan RJ, Derijck AA, Perez-Burgos L *et al*. Partitioning and plasticity of repressive histone methylation states in mammalian chromatin. *Mol Cell* 2003; **12**: 1577–1589.
- 29 Laricchia-Robbio L, Nucifora G. Significant increase of self-renewal in hematopoietic cells after forced expression of EVI1. *Blood Cells Mol Dis* 2008; **40**: 141–147.
- 30 Smith KS, Rhee JW, Cleary ML. Transformation of bone marrow B-cell progenitors by E2a-Hlf requires coexpression of Bcl-2. *Mol Cell Biol* 2002; **22**: 7678–7687.
- 31 Gyory I, Wu J, Fejer G, Seto E, Wright KL. PRDI-BF1 recruits the histone H3 methyltransferase G9a in transcriptional silencing. *Nat Immunol* 2004; **5**: 299–308.
- 32 Greiner D, Bonaldi T, Eskeland R, Roemer E, Imhof A. Identification of a specific inhibitor of the histone methyltransferase SU(VAR)3-9. *Nat Chem Biol* 2005; **1**: 143–145.
- 33 Kubicek S, O'Sullivan RJ, August EM, Hickey ER, Zhang Q, Teodoro ML *et al*. Reversal of H3K9me2 by a small-molecule inhibitor for the G9a histone methyltransferase. *Mol Cell* 2007; **25**: 473–481.

Supplementary Information accompanies the paper on the Leukemia website (<http://www.nature.com/leu>)

ORIGINAL ARTICLE

Pbx1 is a downstream target of Evi-1 in hematopoietic stem/progenitors and leukemic cells

M Shimabe, S Goyama, N Watanabe-Okochi, A Yoshimi, M Ichikawa, Y Imai and M Kurokawa

Department of Hematology and Oncology, Graduate school of Medicine, University of Tokyo, Tokyo, Japan

Ecotropic viral integration site-1 (Evi-1) is a nuclear transcription factor, which is essential for the proliferation/maintenance of hematopoietic stem cells (HSCs). Aberrant expression of Evi-1 has been frequently found in myeloid leukemia, and is associated with a poor patient survival. Recently, we reported candidate target genes of Evi-1 shared in HSCs and leukemic cells using gene expression profiling analysis. In this study, we identified *Pbx1*, a proto-oncogene in hematopoietic malignancy, as a target gene of Evi-1. Overexpression of Evi-1 increased *Pbx1* expression in hematopoietic stem/progenitor cells. An analysis of the *Pbx1* promoter region revealed that Evi-1 upregulates *Pbx1* transcription. Furthermore, reduction of *Pbx1* levels through RNAi-mediated knockdown significantly inhibited Evi-1-induced transformation. In contrast, knockdown of *Pbx1* did not impair bone marrow transformation by E2A/HLF or AML1/ETO, suggesting that *Pbx1* is specifically required for the maintenance of bone marrow transformation mediated by Evi-1. These results indicate that *Pbx1* is a target gene of Evi-1 involved in Evi-1-mediated leukemogenesis.

Oncogene (2009) 28, 4364–4374; doi:10.1038/onc.2009.288; published online 21 September 2009

Keywords: Evi-1; *Pbx1*; leukemogenesis; target gene

Introduction

The ecotropic viral integration site-1 (Evi-1) gene is a member of the SET/PR domain family of transcription factors (Fears *et al.*, 1996; Nitta *et al.*, 2005). It has been shown to interact with several transcriptional regulators like Smad3, CtBP, and PU.1, to mediate transcription (Kurokawa *et al.*, 1998; Izutsu *et al.*, 2001; Laricchia-Robbio *et al.*, 2009). The gene targeting studies in mice revealed that Evi-1 is essential for the proliferation and maintenance of hematopoietic stem cells (HSCs) both during embryogenesis and in the adult (Yuasa *et al.*, 2005; Goyama *et al.*, 2008). Evi-1 regulates HSC proliferation through Gata2 upregulation and repression of

TGF- β signaling in the early hematopoietic development (Yuasa *et al.*, 2005; Sato *et al.*, 2008). In humans, aberrant expression of Evi-1 oncoprotein confers a poor prognosis in hematological malignancies, including acute myeloid leukemia (AML) and myelodysplastic syndrome, particularly in patients with rearrangements on chromosome 3q26, in which Evi-1 is mapped (Pintado *et al.*, 1985; Suzukawa *et al.*, 1994; Ogawa *et al.*, 1996). Overexpression of Evi-1 occurs with high frequency in a subgroup of AML without 3q26 rearrangements, and is also associated with unfavorable outcomes (Barjesteh van Waalwijk van Doorn-Khosrovani *et al.*, 2003; Valk *et al.*, 2004; Lugthart *et al.*, 2008). In murine transplantation model of transformed leukemic cells, disruption of Evi-1 leads to significant loss of their proliferative activity (Goyama *et al.*, 2008). Thus, Evi-1 is a common and critical regulator essential for the proliferation of HSCs and leukemic cells.

Evi-1 contains two DNA-binding zinc finger domains (Perkins *et al.*, 1991; Delwel *et al.*, 1993). Despite the presence of those DNA-binding domains, very few genes have been identified as direct targets of Evi-1 thus far. Gata2 is one of the critical targets for Evi-1 in the early hematopoietic development. Evi-1 was shown to bind directly to Gata2 promoter, and activate its transcription (Yuasa *et al.*, 2005). We earlier revealed candidate target genes of Evi-1 using gene expression profiling analysis in wild-type or Evi-1^{-/-} HSCs combined with the gene expression data of AML samples (Goyama *et al.*, 2008). Genes expressed in the para-aortic splanchnopleural (P-Sp) region of mouse embryos (Gata1, Gata2, and Angpt1), genes involved in the HSC regulation (Gata2, Angpt1, Mpl, Jag2, *Pbx1*, and *Setbp1*), and genes related to platelet formation (Gata1, Mpl, Itga2b, and Itgb3) were identified. Another group also provided set of genes as potential targets for Evi-1 regulation using an inducible EVI1-VP16 chimera, including Gadd45g, Gata2, and Klf5 (Yatsula *et al.*, 2005). Nevertheless, whether those are truly regulated by Evi-1 has yet to be determined.

Here, we have evaluated the potential effect of Evi-1 on *Pbx1* transcription. *Pbx1* is required for the maintenance of definitive hematopoiesis in the fetal liver (FL) and implicated in promoting hematopoietic progenitor cell expansion (DiMartino *et al.*, 2001). In contrast, *Pbx1* is a regulator of HSC self-renewal that contributes to the maintenance of HSC quiescence (Ficara *et al.*, 2008). Thus, *Pbx1* appears to act in a context-dependent manner within the hematopoietic system.

Correspondence: Professor M Kurokawa, Department of Hematology and Oncology, Graduate school of Medicine, University of Tokyo, 7-3-1 Hongo, Bunkyo-ku, Tokyo 113-8655, Japan.

E-mail: kurokawa-tyk@umin.ac.jp

Received 30 April 2009; revised 27 July 2009; accepted 17 August 2009; published online 21 September 2009

In this report, to identify Evi-1 targets, we analyzed those candidate genes and found that Evi-1 binds to Pbx1 promoter and activates Pbx1 transcription. We also showed that RNAi-based knockdown of Pbx1 in Evi-1-transformed progenitors significantly reduced their colony-forming activity. These results indicate that Pbx1 is an important target of Evi-1 involved in Evi-1-mediated leukemogenesis.

Results

Pbx1 expression is transcriptionally regulated by Evi-1

In our earlier report (Goyama *et al.*, 2008), we identified candidate target genes of Evi-1 by comparing gene-expression profiles of wild-type and Evi-1^{-/-} adult HSCs. To narrow down the candidate targets, we first analyzed relative expression of several candidate genes in control- or Evi-1-transduced hematopoietic stem/progenitors. Bone marrow progenitor (cKit⁺) cells were transduced with GFP or Evi-1-GFP-expressing retroviruses, and GFP⁺ cells were sorted (Figure 1a). The low mean intensity of GFP fluorescent is a characteristic feature of cells transduced with Evi-1-expressing retrovirus. Quantitative real-time PCR using the GFP⁺ cells revealed that Evi-1 increased the expression of Pbx1 (mean fold change; 2.50) (Figure 1b). We then assessed the Pbx1 expression in wild-type and Evi-1-deficient FL cells because Evi-1 is required for HSC proliferation in FL (Goyama *et al.*, 2008). As shown in Figure 1c, the expression of Pbx1 is lower in Evi-1-deficient FL cells than that in wild-type FL cells. These results indicate that Pbx1 is a potential candidate gene activated by Evi-1.

To determine whether Evi-1 was directly involved in transcriptional regulation of Pbx1, we next performed luciferase reporter assay. As shown in Figure 1d, the luciferase activity of the Pbx1 reporter plasmid (Pbx1-FL), which includes 3.2 kb upstream of the translational initiation codon (TIC) of Pbx1, showed around two-fold increase over the promoter-less luciferase reporter pGL4.10 (pGL4-Vec). We next generated deletion constructs, and found that deletions ranging from -3.2 to -0.5 kb did not affect activation of the reporter constructs, whereas an internal deletion of the proximal 0.3 kb region completely abolished promoter activity. These results indicate that Pbx1 is a transcriptional target of Evi-1, and the TIC-proximal region (within -0.5 kb) of *Pbx1* gene is necessary for Evi-1-mediated Pbx1 activation.

Identification of functional domains of Evi-1 responsible for *Pbx1* expression

As Evi-1 has several distinct domains with defined biochemical functions (Goyama and Kurokawa, 2009), we next analyzed transcriptional activities of a series of Evi-1 mutants that harbor deletion of the functional domains or substitution of specific residues (Figure 2a). The first zinc-finger domain (1st-ZF) recognizes GA (T/C) AAGA (T/C) AAGATAA consensus sequences *in vitro* (Perkins *et al.*, 1991; Delwel *et al.*, 1993), and is

essential for repressing TGF- β signaling by binding to Smad3 (Kurokawa *et al.*, 1998). The 1st-ZF is also required for inhibiting JNK activity (Kurokawa *et al.*, 2000). The second zinc-finger domain (2nd-ZF) recognizes a consensus sequence of GAAGAT or GATGAG (Funabiki *et al.*, 1994; Yuasa *et al.*, 2005), and is essential for AP-1 activation (Tanaka *et al.*, 1994). The region between amino acid 608 and 732 of Evi-1, which we call the repression domain, is required for the efficient repression of TGF- β signaling, although it does not contribute to binding to Smad3 (Kurokawa *et al.*, 1998). The region containing CtBP-binding-motif-like sequences, PLDLS at amino acid 584, is responsible for the interaction with CtBP1 (Izutsu *et al.*, 2001). In addition, Evi-1 contains a highly acidic domain at the C-terminus, which is required for Evi-1-mediated P-Sp hematopoiesis (Sato *et al.*, 2008). Each construct was transfected into COS7 cells together with D-0.5 reporter construct. As shown in Figure 2a, the deletion including the latter half of the 1st-ZF (Δ ZF5-7, Δ ZF1-7) and the entire 2nd-ZF (Δ ZF8-10, Δ ZF8-10+AD) completely abolishes the reporter activity. Given that Δ ZF5-7 and Δ ZF8-10 still possess some biochemical functions, such as repression ability of TGF- β signaling (Kurokawa *et al.*, 1998), it is unlikely that the diminished reporter activity of these mutants is due to drastic changes in the tertiary and quaternary structures of the protein.

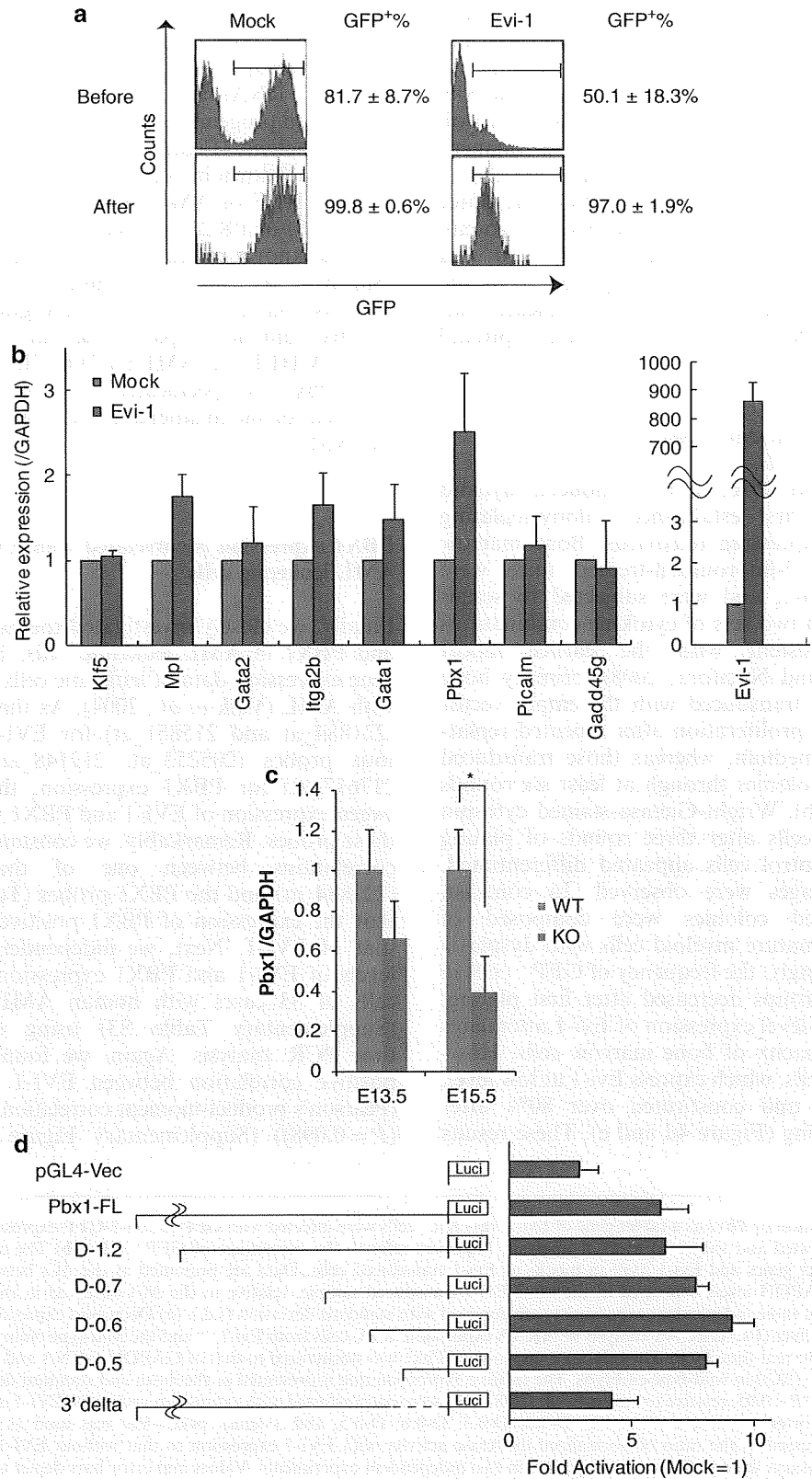
Earlier works have shown that Evi-1 binds directly to DNA through these zinc-finger domains (Perkins *et al.*, 1991; Delwel *et al.*, 1993; Funabiki *et al.*, 1994; Yuasa *et al.*, 2005), we therefore asked whether Evi-1 requires direct sequence-specific DNA binding to induce Pbx1 expression. We found five possible binding sequences for the 1st-ZF (Sites 1, 2, 3, 4, and 6) and one sequence for the 2nd-ZF in this promoter region (Site 5) (Figure 2b), and created promoter constructs that carried mutated Evi-1-binding sites. However, none of these mutations affected the luciferase activity, suggesting that Evi-1 does not require sequence-specific DNA binding to activate Pbx1 (Figure 2c). We also assessed the effect of AP-1 signaling for Pbx1 activation since the 2nd-ZF is essential for AP-1 activation by Evi-1 (Tanaka *et al.*, 1994). The D-0.5 reporter vector was transfected into the COS7 cells together with expression vector c-Jun or AP-1 activator reagent, phorbol 12-myristate 13-acetate (PMA). However, neither c-Jun expression nor PMA addition activated Pbx1 transcription (data not shown). Thus, Evi-1 upregulates Pbx1 expression through both the first and second zinc-finger domains, but the detailed mechanisms underlying Evi-1-mediated Pbx1 activation remain to be elucidated.

EVI-1 binds to PBX1 promoter as a transcriptional regulator in human erythroblast leukemia cells

To determine whether Evi-1 binds to the Pbx1 promoter *in vivo*, we performed a chromatin immunoprecipitation (ChIP) analysis using human erythroblast leukemia (HEL) cells that endogenously express Evi-1 protein. We found that two alternatively spliced variants of

PBX1, PBX1A and PBX1B, were present in HEL cells, with PBX1B appearing as a predominant form (Figure 3a and c). Knockdown of EVI-1 expression

using transient transfection of shRNA (Liu *et al.*, 2006) resulted in a significant decrease in PBX1 mRNA and proteins (both PBX1A and PBX1B) expression, suggest-



ing that PBX1 is regulated by EVI-1 in HEL cells (Figure 3b and c). After the fixation of HEL cells, a sonicated DNA-protein mixture was immunoprecipitated by anti-EVI-1 antibody or Normal Rabbit IgG. The genomic region was amplified by quantitative real-time PCR using primers specific for -354 to -254 bp (-354/-254), -1076 to -960 bp (-1076/-960) and -11277 to -11113 bp (-11277/-11113) upstream regions of PBX1, respectively (Supplementary Table S1). GAPDH promoter region was also used as a control. Among different PBX1 promoter segments, a fragment containing the -354/-254 region, which is located in the homologous region of mouse Pbx1 promoter (D-0.5), bound most robustly to the EVI-1 protein. In contrast, fragments containing -1076/-960 and -11277/-11113 regions were not amplified from the same DNA (Figure 3d). These results indicate that EVI-1 binds to PBX1 promoter as a transcriptional regulator.

Pbx1 is required for efficient propagation of Evi-1-transformed cells

To evaluate a role for Pbx1 in Evi-1-induced myeloid transformation, we first established colony-replating assay using Evi-1-expressing retrovirus. Bone marrow cells derived from 5-fluorouracil-treated mice were transduced with Evi-1, and were subjected to serial-replating assays with two sets of cytokine combinations (Figure 4a). Consistent with the earlier report (Laricchia-Robbio and Nucifora, 2008), primary bone marrow progenitors transduced with the empty vector matured and ceased proliferation after repeated replating in a semisolid medium, whereas those transduced with Evi-1 formed colonies through at least six rounds of plating (Figure 4b). Wright-Giemsa-stained cytopsin preparation of the cells after three rounds of plating showed that the control cells appeared differentiated, and only macrophages were observed. In contrast, the Evi-1-transduced colonies were composed of myeloblasts and immature myeloid cells with dysplasia (Figure 4c). Interestingly, the frequency of GFP⁺ cells in the Evi-1-infected groups decreased after first plating, suggesting that high-level expression of Evi-1 attenuates the proliferating capacity of bone marrow cells. However, the GFP-low cells, which express Evi-1 at low level, gradually increased and constituted over 80% after three rounds of plating (Figure 4d and e). These results

suggest that the relatively low level of expression of Evi-1 confers sustained colony-forming activity in bone marrow cells.

Next, we transduced Pbx1-shRNA or control-shRNA into Evi-1-transduced progenitors after three rounds of plating, and assessed their colony-forming activity (Figure 5a). The inhibitory effect of shRNA on Pbx1 expression was confirmed using NIH3T3 cells (Figure 5b). Of note, RNAi-based knockdown of Pbx1 in Evi-1-transduced progenitors significantly reduced their colony-forming activity (Figure 5c). We then assessed the effect of Pbx1 knockdown in bone marrow progenitors transduced by E2A/HLF or AML1/ETO chimeric genes generated in t(17;19) or t(8;21), respectively. These chimeric genes are also known to transform murine bone marrow cells (Smith *et al.*, 2002; Takeshita *et al.*, 2008), and were used as controls. As shown in Figure 5d, knockdown of Pbx1 did not impair bone marrow transformation by E2A/HLF or AML1/ETO. These results indicate that Pbx1 is specifically, as opposed to generally, required for the maintenance of transformation mediated by Evi-1.

PBX1 expression is correlated with EVI-1 expression in AML leukemic cells

Finally, we closely investigated the expression of EVI-1 and PBX1 in AML leukemic cells. First, we analyzed gene expression data of leukemic cells of 285 individuals with AML (Valk *et al.*, 2004). As there are two probes (221884_at and 215851_at) for EVI-1 expression and four probes (205253_at, 212148_at, 212151_at and 217617_at) for PBX1 expression, the correlation between expression of EVI-1 and PBX1 was assessed using these probes. Remarkably, we constantly found positive correlations between one of the EVI-1 probes (221884_at) and the PBX1 probes (Table 1), suggesting that the expression of PBX1 positively correlates with that of EVI-1. Next, we independently examined the levels of EVI-1 and PBX1 expression in bone marrow cells of 33 cases with human AML in our institute (Supplementary Table S3) using quantitative real-time PCR analysis. Again, we found a tendency for positive correlation between EVI-1 and PBX1 levels (Pearson's product-moment correlation coefficient = 0.293 ($P=0.098$)) (Supplementary Figure S1). These data

Figure 1 Identification of *Pbx1* as a target gene of Evi-1. (a) cKit⁺ cells were infected with GFP or Evi-1-GFP-expressing retroviruses. GFP⁺ cells were sorted and subjected to PCR analysis. Numbers refer to the percentage of GFP⁺ cells. (b) The expression of the putative Evi-1 target genes and Evi-1 itself in mock- or Evi-1 transduced cells. Data are presented as the ΔC_t between the gene of interest and the GAPDH levels expressed in the same Evi-1-transduced sample, relative to the ΔC_t observed in the paired control sample. Means from three independent experiments are depicted with standard deviation (s.d.). (c) Decreased expression of Pbx1 gene in the Evi-1^{-/-} fetal liver (FL) cells. An analysis of mRNA expression in FL cells from Evi-1^{-/-} and the wild-type embryos at E13.5 and E15.5 by quantitative real-time PCR. The mRNA expression of Pbx1 was normalized to that of GAPDH mRNA and calibrated to the Pbx1/GAPDH ratio (ΔC_t) in wild-type embryos. The relative expression rate is presented as the mean and standard deviation of $2^{-\Delta\Delta C_t}$ in triplicate assays. * $P < 0.05$, relative to controls. (d) COS7 cells were cotransfected with expression vector for EVI-1 and various Pbx1 promoter-LUC reporter constructs (Pbx1-FL, D-1.2, D-0.7, D-0.6, D-0.5, and 3'delta). pGL4-Vec was used as a control. Fold activation was expressed as the ratio of normalized luciferase activity with EVI-1 expression to that without EVI-1 expression. All luciferase reporter assays were performed in duplicate in two independent experiments. Values and error bars depict the mean and the s.d., respectively. Dash indicates the deleted region in the construct.

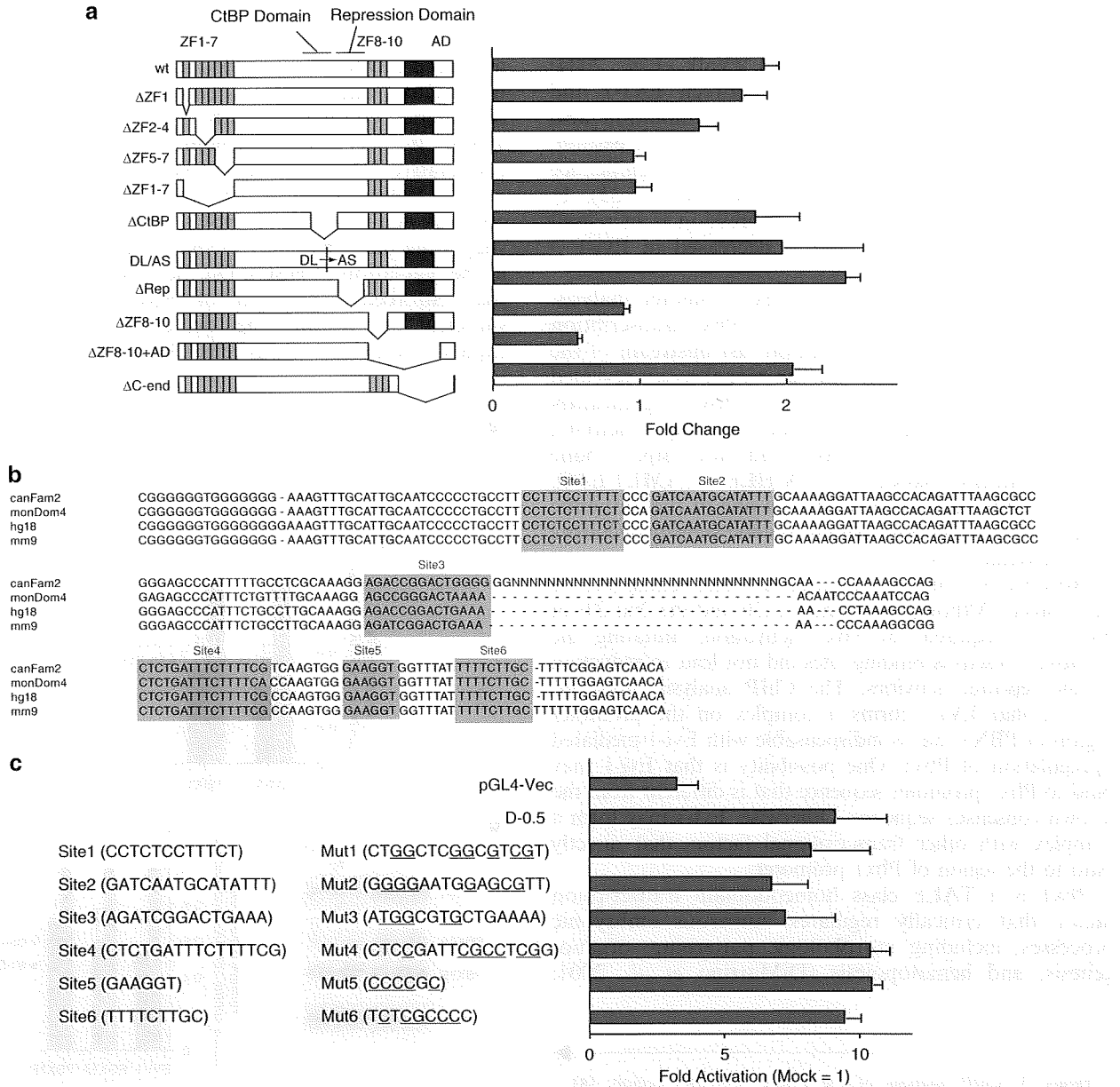


Figure 2 Identification of functional domains of Evi-1 responsible for Pbx1 expression. (a) Structures of wild-type EVI-1 (wt) and mutants are depicted. ZF, zinc-finger motif; AD, the acidic domain. Zinc-finger motifs are numbered 1–10. DL/AS mutant has a point mutation that abolishes CtBP binding. COS7 cells were cotransfected with D-0.5 reporter vector and each expression vector for EVI-1 (wt) or EVI-1 mutants (Δ ZF1, Δ ZF2–4, Δ ZF5–7, Δ ZF1–7, Δ CtBP, DL/AS, Δ Rep, Δ ZF8–10, Δ ZF8–10 + AD, and Δ C-end). Fold change was calculated by dividing the fold activation of each EVI-1 mutant cotransfected with D-0.5 by the fold activation of the respective EVI-1 mutant cotransfected with pGL4-Vec. All luciferase reporter assays were performed in duplicate in two independent experiments. Values and error bars depict the mean and the s.d., respectively. (b) Multiple sequence alignments of the region flanking the Pbx1 TIC. Predicted conserved Evi-1-binding sites are indicated. (c) Reporter plasmids containing either the wild-type promoter (D-0.5) or the indicated mutants were transiently transfected into COS7 cells and EVI-1 responsiveness was assayed. All luciferase reporter assays were performed in duplicate in two independent experiments. Values and error bars depict the mean and s.d., respectively.

suggest that the correlation between EVI-1 and PBX1 exists in human AML.

Discussion

Despite the established role of Evi-1 in leukemia development, molecular mechanisms underlying Evi-1-

mediated leukemogenesis remain elusive. Especially, very few genes have been identified as downstream targets of Evi-1 thus far. In this study, we report a novel Evi-1-regulated gene, *Pbx1*. Several approaches were used to show that Pbx1 is a target of Evi-1. First, we combined gene-expression-profiling analysis in wild-type or Evi-1^{-/-} HSCs with the gene-expression data of AML samples, and found that the expression of Pbx1

correlates with that of Evi-1 in both HSCs and AML cells (Goyama *et al.*, 2008). Analysis of gene expression data of 285 individuals with AML (Valk *et al.*, 2004) showed the positive correlation between EVI-1 and PBX1 expression. Our independent examination also showed a tendency toward positive correlation, although, it did not reach statistical significance probably due to the limited sample size ($n=33$). In addition, we showed that Pbx1 expression is increased by Evi-1 overexpression and is decreased in Evi-1^{-/-} FL cells.

Second, through an extensive Pbx1 promoter analysis, we showed that Evi-1 regulates the Pbx1 transcription by binding to the proximal region just upstream of the Pbx1 TIC. Furthermore, our functional assay revealed that RNAi-based knockdown of Pbx1 significantly inhibited Evi-1-induced colony-forming activity, whereas knockdown of Pbx1 did not impair bone marrow transformation by E2A/HLF or AML1/ETO. These results indicate that Pbx1 is one of the authentic targets of Evi-1 in both hematopoietic stem/progenitors and leukemic cells.

How Evi-1 achieves activation of Pbx1 remains to be determined. Although both the 1st-ZF and the 2nd-ZF of Evi-1 are required for Pbx1 activation, mutating the putative consensus-binding sites did not lead to reduction of the reporter activities. The ChIP analysis, however, showed that EVI-1 forms a complex on the promoter region of PBX1 that is indispensable with Evi-1-mediated upregulation of Pbx1. One possibility is that Evi-1 may bind to Pbx1 promoter sequence that is different from the known consensus sequence. Otherwise, Evi-1 may form a complex with other transcriptional factors that directly bind to the region of Pbx1 promoter.

Pbx1 is a TALE class homeodomain transcription factor that critically regulates numerous embryonic processes, including morphologic patterning, organogenesis, and hematopoiesis (DiMartino *et al.*, 2001;

Selleri *et al.*, 2001; Kim *et al.*, 2002; Schnabel *et al.*, 2003; Manley *et al.*, 2004). It enhances the relatively nonspecific DNA-binding properties of Hox transcription factors and regulates gene expression as hetero-oligomeric complexes with Hox proteins (Mann, 1995). It acts as a protein partner to facilitate cooperative DNA binding by Hox proteins (Lawrence *et al.*, 1996). Recently, it was reported that Pbx1 controls self-renewal of HSCs (Ficara *et al.*, 2008), suggesting that Pbx1 may mediate the function of Evi-1 in the regulation of HSCs. On the other hand, we found that enforced expression of Pbx1 alone was not sufficient to restore the decreased colony-forming capacity of Evi-1^{-/-} P-Sp cells (data not shown). These

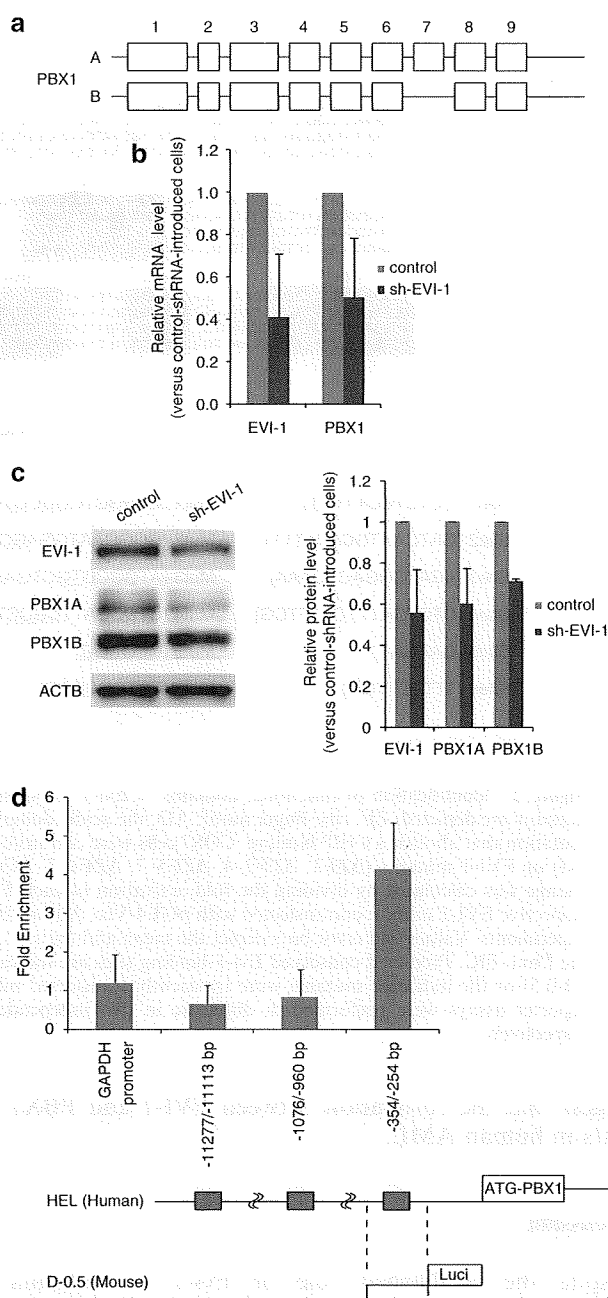
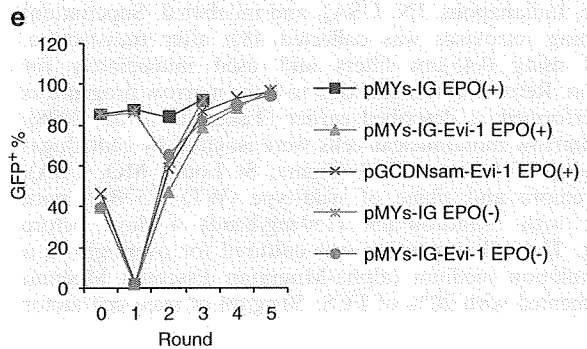
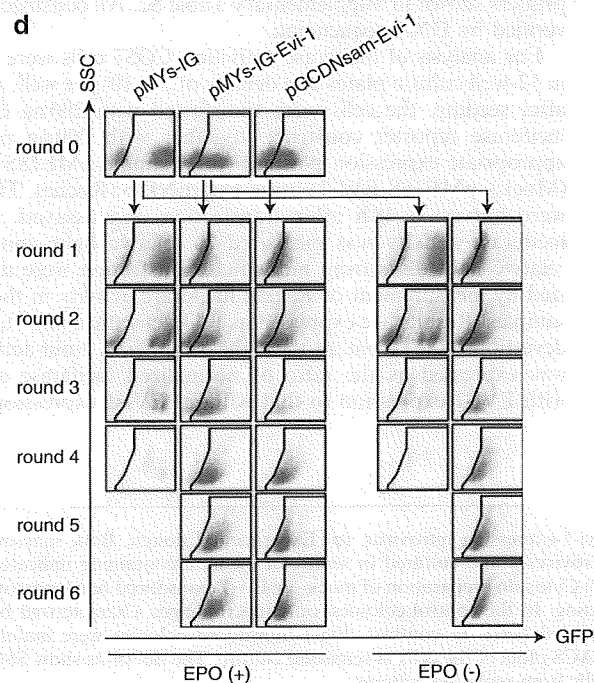
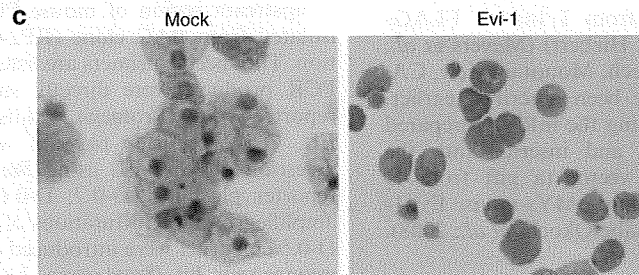
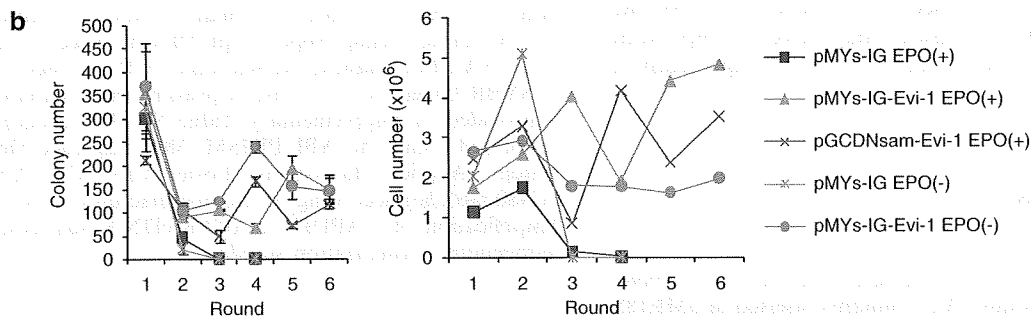
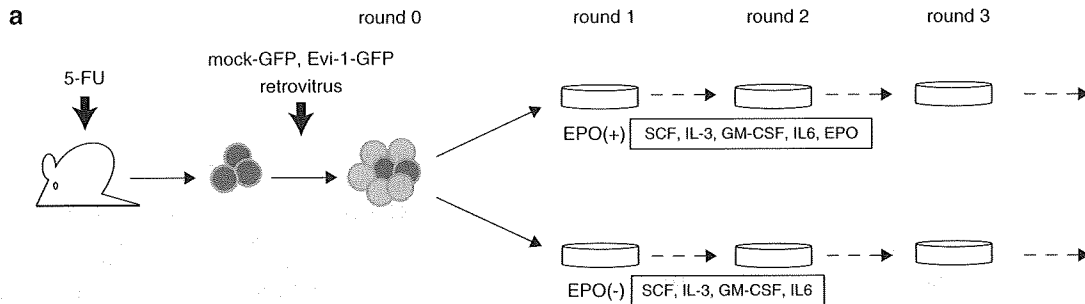


Figure 3 ChIP analysis of the PBX1 promoter region. (a) Schematic representation of genomic structure of PBX1A and PBX1B splicing isoforms. (b) Quantitative real-time PCR analysis showed that shRNA interference downregulates EVI-1 expression in HEL cells, which resulted in downregulation of PBX1 expression. The bar graph represents normalized expression of EVI-1 and PBX1 mRNA. Results are expressed as the mean and s.d. for three experiments. (c) Western blotting showed that shRNA interference downregulates EVI-1 expression in HEL cells, which resulted in downregulation of PBX1 expression (left). Relative protein levels of EVI-1, PBX1A, and PBX1B normalized to ACTB are shown in the right panel. Results are expressed as the mean and s.d. for three experiments. (d) Specific DNA binding of EVI-1 to -354/-254 bp region detected by ChIP. Real-time PCR was performed on fragmented chromatin precipitated by Normal Rabbit IgG or an anti-EVI-1 antibody from HEL cells. PCR primers were designed to amplify three different regions at PBX1 promoter (-11277/-11113 bp, -1076/-960 bp, and -354/-254 bp). Primer designed to amplify GAPDH promoter region was used as a control. Results were presented as the fold enrichment of chromatin DNA precipitated by the anti-EVI-1 antibody to control chromatin DNA precipitated by Normal Rabbit IgG. Columns, mean of triplicate experiments; bars, s.d.

results suggest that Pbx1 might need other target gene products of Evi-1 to rescue the hematopoietic defects of Evi-1-deficient cells.

Pbx1 has also been implicated in the development of several tumors including hematological malignancies (Kamps *et al.*, 1990, 1991; Nourse *et al.*, 1990; Qiu *et al.*,



2007; Shiraishi *et al.*, 2007; Park *et al.*, 2008). It is required for the execution of some Hox-dependent block of differentiation, and/or transformation (Krosi *et al.*, 1998; Knoepfler *et al.*, 2001; Yaron *et al.*, 2001), and mutations of HoxA9 that prevent interaction with Pbx proteins abrogate its oncogenic properties (Schnabel *et al.*, 2000). Notably, Evi-1 also cooperates with Hoxa and Meis1 in myeloid leukemogenesis (Jin *et al.*, 2007). Therefore, together with the findings in this report, the Evi-1-Pbx1 pathway may cooperate with Hox proteins for leukemia development.

In summary, we showed that Evi-1 binds to the Pbx1 promoter and activates its expression. Aberrant expression of Pbx1 is responsible, at least in part, for the leukemogenic activity of Evi-1. Given that both Evi-1 and Pbx1 are highly expressed in a variety of tumors, the role of the Evi-1-Pbx1 pathway may have an important function for cancer development in a broad spectrum of tissues.

Materials and methods

DNA constructs

The plasmid pME18S-EVI-1 (human) (Tanaka *et al.*, 1994; Nitta *et al.*, 2005), various EVI-1 mutants inserted in pME18S (Tanaka *et al.*, 1994; Kurokawa *et al.*, 1998; Izutsu *et al.*, 2001), pMXs-neo-E2A/HLF (a gift from T Inaba), FLAG-tagged-AML1/ETO (a gift from SW Hiebert) (Meyers *et al.*, 1993) inserted in pMSCV-neo (Clontech, Mountain view, CA, USA) (Takeshita *et al.*, 2008), have been described earlier. Mouse Evi-1 cDNA was obtained using the mRNA prepared from P-Sp region of the embryo, and inserted into the pGCDNsam-IRES-eGFP retroviral vector (a gift from H Nakauchi and M Onodera). The plasmid pMYs-mouse Evi-1-IG has been described earlier (Watanabe-Okochi *et al.*, 2008).

Retroviral transduction

To obtain retrovirus supernatants, 8×10^5 Plat-E packaging cells per 6-cm culture dish were transiently transfected with 3 μ g of each retrovirus vector, mixed with 9 μ L of FuGENE 6 (Roche, Indianapolis, IN, USA), and incubated. Supernatant containing retrovirus was collected 48 h after transfection, filtered using 0.45- μ m filters and used immediately for infection. Retroviral transduction to bone marrow progenitors was performed as described earlier (Takeshita *et al.*, 2008). Bone marrow mononuclear cells were isolated by centrifugation using Histopaque 1083 (Sigma, St Louis, MO, USA), from femora and tibiae of wild-type (WT) C57Bl/6 mice treated with 5-fluorouracil (150 mg/head) 4 days before harvest. The cell suspension was cultured for overnight in a prestimulation medium (alpha-Minimum Essential Medium supplemented with 20% of FCS, 50 ng/ml of stem cell factor

(SCF; Wako, Osaka, Japan), Flt3-ligand (Flt3 L; R&D, Minneapolis, MN, USA), thrombopoietin and a fusion protein of IL-6R and IL-6). After stimulation, cells were harvested and seeded with retroviral supernatants on RetroNectin (Takara Bio, Otsu, Japan) coated dishes.

Quantitative real-time PCR analysis

cKit⁺ bone marrow mononuclear cells were isolated with anti-CD117 (cKit) magnetic beads and using the AutoMACS apparatus (Miltenyi Biotec, Bergisch Gladbach, Germany) according to the manufacturer's instructions. pGCDNsam-mouse Evi-1-IRES-eGFP or pGCDNsam-IRES-eGFP retrovirus was introduced into cKit⁺ bone marrow progenitors. Total RNA was extracted from the GFP⁺ bone marrow progenitors sorted by a FACSAria cell sorter (BD Biosciences, San Jose, CA, USA), FL cells and HEL cells using RNeasy Mini kit (Qiagen, Hilden, Germany). Reverse transcription was performed using SuperScript III (Invitrogen, Carlsbad, CA, USA). For quantitative real-time PCR, we used Taqman or SYBR Green assays. A list of primers and Taqman probes is provided in Supplementary Table S1. All reactions were performed using the ABI PRISM 7000 Sequence Detection System (Applied Biosystems, Foster City, CA, USA) or LC480 (Roche) according to the manufacturer's instructions. Amplification of GAPDH or ACTB cDNA was used as the endogenous normalization standard.

Reporter gene constructs and luciferase reporter assay

5' upstream region of mouse Pbx1 (-3247 to -179 bp) was isolated from BAC clone (RP24-243I12) by PCR amplification. The specific primers are listed in Supplementary Table S1. PCR products were directly subcloned into the pGL4.10 reporter vector (Promega, Madison, WI, USA), named Pbx1-FL. D-1.2 reporter plasmid was generated by restriction digestion of Pbx1-FL using *Bam*HI and *Eco*RV. The other reporter plasmids (D-0.7, D-0.6, D-0.5, and 3' delta) were amplified by PCR. Mutations of the Evi-1 recognition sites in D-0.5 construct were introduced by QuickChange site-directed mutagenesis kit (Stratagene, La Jolla, CA, USA) using the primers shown in Supplementary Table S2. All constructs were verified by DNA sequencing.

For analysis of luciferase activities, COS7 cells were seeded in 12-well culture plates at a density of 2×10^4 per well. At 12 h after seeding, the cells were transfected with 200 ng of each luciferase reporter construct, together with 200 ng of each appropriate expression plasmid (for example pME18S vector (Mock), pME18S-EVI-1) using FuGENE 6 (Roche). The cells were harvested 48 h after transfection and assayed. Firefly luciferase activity was measured as relative light units. The relative light units from individual transfection were normalized by measurement of *Renilla* luciferase activity in the same samples. Results are expressed as fold activation and standard deviations (s.d.) from all these measurements. Fold activation was expressed as the ratio of normalized luciferase activity with EVI-1 expression to that without EVI-1 expression.

Figure 4 Colony replating capacity of the cells infected with Evi-1-expressing retrovirus. (a) Experimental design. Bone marrow progenitors were infected with GFP or Evi-1-GFP-expressing retroviruses and cultured in semisolid medium containing indicated cytokines. (b) Colony and cell counts from the replating cultures. (c) Cytospin preparation of mock- or Evi-1-transduced bone marrow progenitors stained with Wright-Giemsa after three rounds of plating. In the control colonies, only macrophages, characterized by small compact nuclei and large vacuolated cytoplasm, were observed (left). In contrast, Evi-1-transduced colonies were mainly composed of myeloblasts and immature myeloid cells (right). (d) FACS plots of the cells in semisolid culture. The dot plots show SSC (*y* axis) versus GFP intensity (*x* axis). (e) Percentages of GFP⁺ cells from replating cultures.

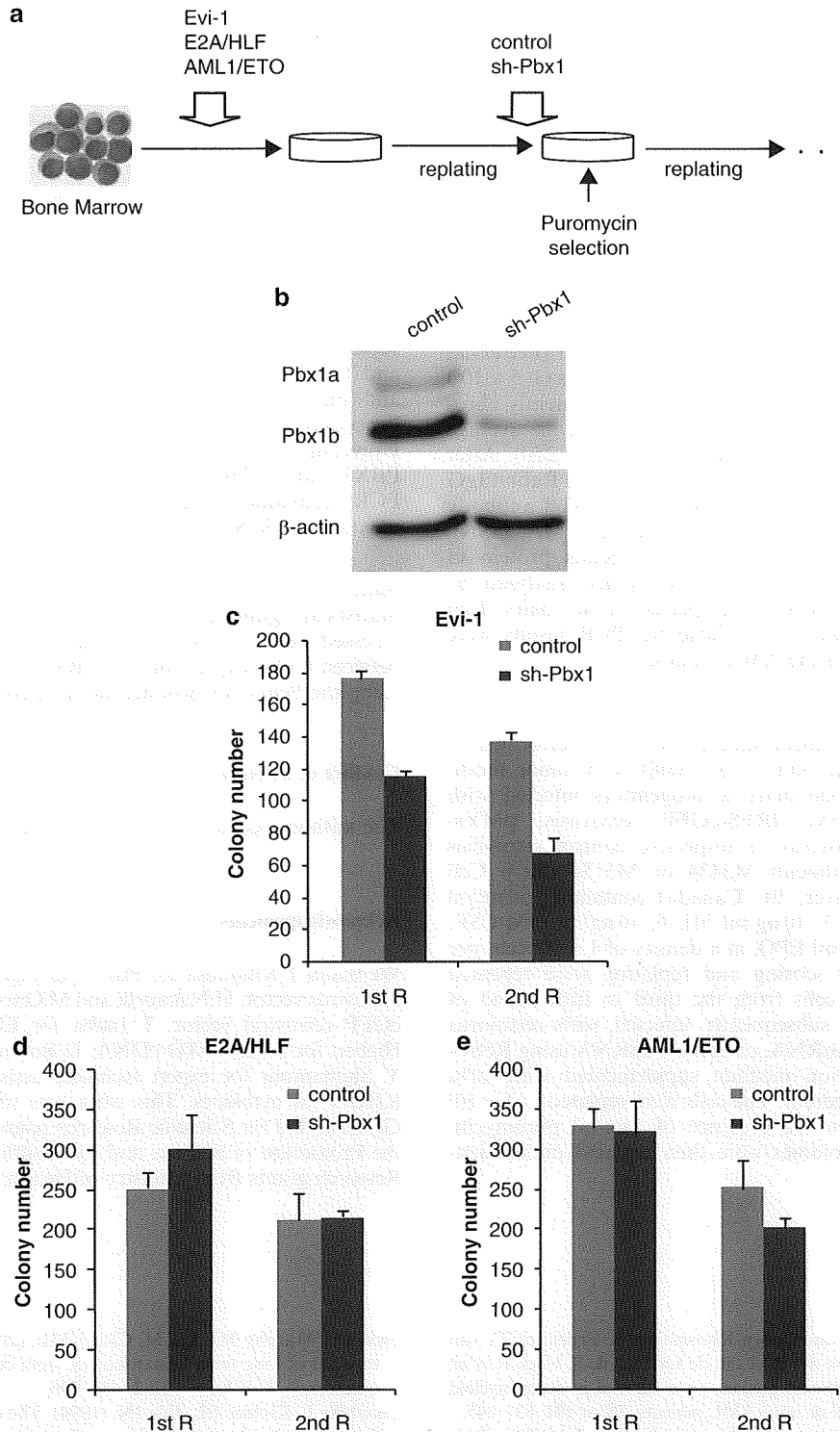


Figure 5 Effects of Pbx1 knockdown on myeloid transformation. (a) Schematic representation of following experiments. BM progenitors were transduced with Evi-1, E2A/HLF, or AML1/ETO oncogenes. Transformed cells from the third to fifth round of *in vitro* plating were subsequently transduced with Pbx1-shRNA or control-shRNA, and puromycin-resistant colonies were selected. Clonogenic activity was then assessed in the further round of replating in the presence of puromycin. (b) Western blotting showed that shRNA interference effectively downregulates both Pbx1a and Pbx1b expression in NIH3T3 cells. Expression of β-actin was also shown as controls. (c) Counts of puromycin-resistant colonies from the replating cultures of Evi-1-transformed cells after sh-RNA transduction. The bar graph shows the numbers of colonies obtained after each round of replating in the methylcellulose (mean ± s.d.). The representative data of two independent experiments in duplicate are shown. (d, e) Counts of puromycin-resistant colonies from the replating cultures of E2A/HLF-transformed cells or AML1/ETO-transformed cells after sh-RNA transduction. The bar graph shows the numbers of colonies obtained after each round of replating in the methylcellulose (mean ± s.d.). The representative data of two independent experiments in duplicate are shown.

Table 1 Pearson's product-moment correlation coefficient between EVI-1 and PBX1 expression in 285 AML

PBX1 probe	EVI-1 probe: 221884_at		EVI-1 probe: 215851_at	
	r	P	r	P
205253_at	0.156	0.008	0.107	0.072
212148_at	0.135	0.023	0.040	0.500
212151_at	0.139	0.019	0.032	0.588
217617_at	0.125	0.035	0.077	0.195

ChIP assay

A ChIP analysis was performed as described earlier (Lee *et al.*, 2006), with minor modifications. Briefly, HEL cells ($1-5 \times 10^7$) were crosslinked with 1% formaldehyde. Subsequently chromatin was fragmented by sonication to obtain an average fragment length of 200–900 bp (Bronson Sonifier 250). After the chromatin fraction was incubated with Normal Rabbit IgG (Abcam Inc., Cambridge, MA, USA) or anti-EVI-1 antibody (#C50E12; Cell Signaling Technology, Danvers, MA, USA), immune complexes were bound to Dynabeads protein G (Invitrogen). Eluted DNA samples were then analyzed by quantitative real-time PCR using specific primer pairs (Lim *et al.*, 2005) in Supplementary Table S1. PCR results were calculated validly using the $\Delta\Delta C_t$ method.

Myeloid progenitor transformation assay

Myeloid progenitor transformation assay was performed as described earlier (Takeshita *et al.*, 2008) with minor modifications. In brief, bone marrow progenitors infected with pGCDNsam-mouse Evi-1-IRES-eGFP retrovirus, pMys-mouse Evi-1 IG retrovirus or respective control retrovirus were cultured in Methocult M3434 or M3134 (Stem Cell Technologies, Vancouver, BC Canada) containing 50 ng/ml mSCF, 10 ng/ml mL-3, 10 ng/ml hIL-6, 10 ng/ml GM-CSF, with or without 3 unit/ml EPO, at a density of 1×10^4 cells per 35-mm plate. Colony scoring and replating were repeated weekly. Transformed cells from the third to fifth round of *in vitro* plating were subsequently infected with retrovirus encoding either Pbx1-shRNA, or control-shRNA using RetroNectin in prestimulation medium supplemented with 10% WEHI conditioned medium. The cells were replated at 1×10^5 per plate in M3434 in the presence of 1 μ g/ml puromycin. Puromycin-resistant colonies were then replated under identical conditions.

References

- Barjesteh van Waalwijk van Doorn-Khosrovani S, Erpelinck C, van Putten WL, Valk PJ, van der Poel-van de Luytgaarde S, Hack R *et al.* (2003). High EVI1 expression predicts poor survival in acute myeloid leukemia: a study of 319 *de novo* AML patients. *Blood* **101**: 837–845.
- Delwel R, Funabiki T, Kreider BL, Morishita K, Ihle JN. (1993). Four of the seven zinc fingers of the Evi-1 myeloid-transforming gene are required for sequence-specific binding to GA(C/T)AAGA(T/C)AA GATAA. *Mol Cell Biol* **13**: 4291–4300.
- DiMartino JF, Selleri L, Traver D, Firpo MT, Rhee J, Warnke R *et al.* (2001). The Hox cofactor and proto-oncogene Pbx1 is required for maintenance of definitive hematopoiesis in the fetal liver. *Blood* **98**: 618–626.
- Fears S, Mathieu C, Zeleznik-Le N, Huang S, Rowley JD, Nucifora G. (1996). Intergenic splicing of MDS1 and EVI1 occurs in normal tissues as well as in myeloid leukemia and produces a new member of the PR domain family. *Proc Natl Acad Sci USA* **93**: 1642–1647.
- Ficara F, Murphy MJ, Lin M, Cleary ML. (2008). Pbx1 regulates self-renewal of long-term hematopoietic stem cells by maintaining their quiescence. *Cell Stem Cell* **2**: 484–496.
- Funabiki T, Kreider BL, Ihle JN. (1994). The carboxyl domain of zinc fingers of the Evi-1 myeloid transforming gene binds a consensus sequence of GAAGATGAG. *Oncogene* **9**: 1575–1581.
- Goyama S, Kurokawa M. (2009). Pathogenetic significance of ecotropic viral integration site-1 in hematological malignancies. *Cancer Sci* **100**: 990–995.
- Goyama S, Yamamoto G, Shimabe M, Sato T, Ichikawa M, Ogawa S *et al.* (2008). Evi-1 is a critical regulator for hematopoietic stem cells and transformed leukemic cells. *Cell Stem Cell* **3**: 207–220.
- Itzutsu K, Kurokawa M, Imai Y, Maki K, Mitani K, Hirai H. (2001). The corepressor CtBP interacts with Evi-1 to repress transforming growth factor beta signaling. *Blood* **97**: 2815–2822.

Clinical samples

To elucidate the level of PBX1 expression in clinical samples, we used gene expression data of 285 individuals with AML (www.ncbi.nlm.gov/geo, accession number GSE1159 [NCBI GEO]) (Valk *et al.*, 2004). Normalization and expression values of the microarray data were calculated using the statistical language R (<http://www.bioconductor.org>).

We independently analyzed bone marrow samples from 33 AML patients (Supplementary Table S3) after obtaining written informed consent. Studies involving human subjects were done in accordance with the ethical guidelines for biomedical research involving human subjects, which was developed by the Ministry of Health, Labour and Welfare, Japan, the Ministry of Education, Culture, Sports, Science, and Technology, Japan, and the Ministry of Economy, Trade, and Industry, Japan, and enforced 24 on March 29, 2001. Procedures were approved by ethical committee of Tokyo University. The expression of EVI-1 (Primer; EVI-1 SYBR), PBX1 and ACTB were measured using quantitative real-time PCR techniques. The specific primers are listed in Supplementary Table S1.

Statistical analysis

Statistical significance of differences between parameters was assessed using a two-tailed paired *t* test. The correlation between EVI-1 expression and PBX1 expression was estimated using the Pearson's product-moment correlation coefficient.

Conflict of interest

The authors declare no conflict of interest.

Acknowledgements

We thank T Kitamura for Plat-E packaging cells and pMys-IG retrovirus vector, H Nakauchi and M Onodera for pGCDNsam-eGFP retroviral vector, T Inaba for E2A/HLF cDNA, SW Hiebert for AML1/ETO cDNA, D Bohmann for c-Jun cDNA, Y Shimamura for expert technical assistance, and KYOWA KIRIN for cytokines. This work was supported in part by a Grant-in-Aid for Scientific Research from the Japan Society for the Promotion of Science, and by Health and Labour Sciences Research grants from Ministry of Health, Labour and Welfare.

- Jin G, Yamazaki Y, Takuwa M, Takahara T, Kaneko K, Kuwata T *et al.* (2007). Trib1 and Evi1 cooperate with Hoxa and Meis1 in myeloid leukemogenesis. *Blood* **109**: 3998–4005.
- Kamps MP, Look AT, Baltimore D. (1991). The human t(1;19) translocation in pre-B ALL produces multiple nuclear E2A-Pbx1 fusion proteins with differing transforming potentials. *Genes Dev* **5**: 358–368.
- Kamps MP, Murre C, Sun XH, Baltimore D. (1990). A new homeobox gene contributes the DNA binding domain of the t(1;19) translocation protein in pre-B ALL. *Cell* **60**: 547–555.
- Kim SK, Selleri L, Lee JS, Zhang AY, Gu X, Jacobs Y *et al.* (2002). Pbx1 inactivation disrupts pancreas development and in *Ipfl*-deficient mice promotes diabetes mellitus. *Nat Genet* **30**: 430–435.
- Knoepfler PS, Sykes DB, Pasillas M, Kamps MP. (2001). HoxB8 requires its Pbx-interaction motif to block differentiation of primary myeloid progenitors and of most cell line models of myeloid differentiation. *Oncogene* **20**: 5440–5448.
- Kros J, Baban S, Kros G, Rozenfeld S, Largman C, Sauvageau G. (1998). Cellular proliferation and transformation induced by HOXB4 and HOXB3 proteins involves cooperation with PBX1. *Oncogene* **16**: 3403–3412.
- Kurokawa M, Mitani K, Irie K, Matsuyama T, Takahashi T, Chiba S *et al.* (1998). The oncoprotein Evi-1 represses TGF- β signalling by inhibiting Smad3. *Nature* **394**: 92–96.
- Kurokawa M, Mitani K, Yamagata T, Takahashi T, Izutsu K, Ogawa S *et al.* (2000). The *evi-1* oncoprotein inhibits c-Jun N-terminal kinase and prevents stress-induced cell death. *EMBO J* **19**: 2958–2968.
- Laricchia-Robbio L, Nucifora G. (2008). Significant increase of self-renewal in hematopoietic cells after forced expression of EVI1. *Blood Cells Mol Dis* **40**: 141–147.
- Laricchia-Robbio L, Premanand K, Rinaldi CR, Nucifora G. (2009). EVI1 impairs myelopoiesis by deregulation of PU.1 function. *Cancer Res* **69**: 1633–1642.
- Lawrence HJ, Sauvageau G, Humphries RK, Largman C. (1996). The role of HOX homeobox genes in normal and leukemic hematopoiesis. *Stem Cells* **14**: 281–291.
- Lee TI, Johnstone SE, Young RA. (2006). Chromatin immunoprecipitation and microarray-based analysis of protein location. *Nat Protoc* **1**: 729–748.
- Lim JH, Booker AB, Luo T, Williams T, Furuta Y, Lagutin O *et al.* (2005). AP-2 α selectively regulates fragile X mental retardation-1 gene transcription during embryonic development. *Hum Mol Genet* **14**: 2027–2034.
- Liu Y, Chen L, Ko TC, Fields AP, Thompson EA. (2006). Evi1 is a survival factor which conveys resistance to both TGF β and taxol-mediated cell death via PI3K/AKT. *Oncogene* **25**: 3565–3575.
- Lugthart S, van Drunen E, van Norden Y, van Hoven A, Erpelinck CA, Valk PJ *et al.* (2008). High EVI1 levels predict adverse outcome in acute myeloid leukemia: prevalence of EVI1 overexpression and chromosome 3q26 abnormalities underestimated. *Blood* **111**: 4329–4337.
- Manley NR, Selleri L, Brendolan A, Gordon J, Cleary ML. (2004). Abnormalities of caudal pharyngeal pouch development in Pbx1 knockout mice mimic loss of Hox3 paralogs. *Dev Biol* **276**: 301–312.
- Mann RS. (1995). The specificity of homeotic gene function. *Bioessays* **17**: 855–863.
- Meyers S, Downing JR, Hiebert SW. (1993). Identification of AML-1 and the (8;21) translocation protein (AML-1/ETO) as sequence-specific DNA-binding proteins: the runt homology domain is required for DNA binding and protein-protein interactions. *Mol Cell Biol* **13**: 6336–6345.
- Nitta E, Izutsu K, Yamaguchi Y, Imai Y, Ogawa S, Chiba S *et al.* (2005). Oligomerization of Evi-1 regulated by the PR domain contributes to recruitment of corepressor CtBP. *Oncogene* **24**: 6165–6173.
- Nourse J, Mellentin JD, Galili N, Wilkinson J, Stanbridge E, Smith SD *et al.* (1990). Chromosomal translocation t(1;19) results in synthesis of a homeobox fusion mRNA that codes for a potential chimeric transcription factor. *Cell* **60**: 535–545.
- Ogawa S, Kurokawa M, Tanaka T, Mitani K, Inazawa J, Hangaishi A *et al.* (1996). Structurally altered Evi-1 protein generated in the 3q21q26 syndrome. *Oncogene* **13**: 183–191.
- Park JT, Shih Ie M, Wang TL. (2008). Identification of Pbx1, a potential oncogene, as a Notch3 target gene in ovarian cancer. *Cancer Res* **68**: 8852–8860.
- Perkins AS, Fishel R, Jenkins NA, Copeland NG. (1991). Evi-1, a murine zinc finger proto-oncogene, encodes a sequence-specific DNA-binding protein. *Mol Cell Biol* **11**: 2665–2674.
- Pintado T, Ferro MT, San Roman C, Mayayo M, Larana JG. (1985). Clinical correlations of the 3q21;q26 cytogenetic anomaly. A leukemic or myelodysplastic syndrome with preserved or increased platelet production and lack of response to cytotoxic drug therapy. *Cancer* **55**: 535–541.
- Qiu Y, Tomita Y, Zhang B, Nakamichi I, Morii E, Aozasa K. (2007). Pre-B-cell leukemia transcription factor 1 regulates expression of valosin-containing protein, a gene involved in cancer growth. *Am J Pathol* **170**: 152–159.
- Sato T, Goyama S, Nitta E, Takeshita M, Yoshimi M, Nakagawa M *et al.* (2008). Evi-1 promotes para-aortic splanchnopleural hematopoiesis through up-regulation of GATA-2 and repression of TGF- β signaling. *Cancer Sci* **99**: 1407–1413.
- Schnabel CA, Godin RE, Cleary ML. (2003). Pbx1 regulates nephrogenesis and ureteric branching in the developing kidney. *Dev Biol* **254**: 262–276.
- Schnabel CA, Jacobs Y, Cleary ML. (2000). HoxA9-mediated immortalization of myeloid progenitors requires functional interactions with TALE cofactors Pbx and Meis. *Oncogene* **19**: 608–616.
- Selleri L, Depew MJ, Jacobs Y, Chanda SK, Tsang KY, Cheah KS *et al.* (2001). Requirement for Pbx1 in skeletal patterning and programming chondrocyte proliferation and differentiation. *Development* **128**: 3543–3557.
- Shiraishi K, Yamasaki K, Nanba D, Inoue H, Hanakawa Y, Shirakata Y *et al.* (2007). Pre-B-cell leukemia transcription factor 1 is a major target of promyelocytic leukemia zinc-finger-mediated melanoma cell growth suppression. *Oncogene* **26**: 339–348.
- Smith KS, Rhee JW, Cleary ML. (2002). Transformation of bone marrow B-cell progenitors by E2a-Hlf requires coexpression of Bcl-2. *Mol Cell Biol* **22**: 7678–7687.
- Suzukawa K, Parganas E, Gajjar A, Abe T, Takahashi S, Tani K *et al.* (1994). Identification of a breakpoint cluster region 3' of the ribophorin I gene at 3q21 associated with the transcriptional activation of the EVI1 gene in acute myelogenous leukemias with inv(3)(q21q26). *Blood* **84**: 2681–2688.
- Takeshita M, Ichikawa M, Nitta E, Goyama S, Asai T, Ogawa S *et al.* (2008). AML1-Evi-1 specifically transforms hematopoietic stem cells through fusion of the entire Evi-1 sequence to AML1. *Leukemia* **22**: 1241–1249.
- Tanaka T, Nishida J, Mitani K, Ogawa S, Yazaki Y, Hirai H. (1994). Evi-1 raises AP-1 activity and stimulates c-fos promoter transactivation with dependence on the second zinc finger domain. *J Biol Chem* **269**: 24020–24026.
- Valk PJ, Verhaak RG, Beijnen MA, Erpelinck CA, Barjesteh van Waalwijk van Doorn-Khosrovani S, Boer JM *et al.* (2004). Prognostically useful gene-expression profiles in acute myeloid leukemia. *N Engl J Med* **350**: 1617–1628.
- Watanabe-Okochi N, Kitaura J, Ono R, Harada H, Harada Y, Komeno Y *et al.* (2008). AML1 mutations induced MDS and MDS/AML in a mouse BMT model. *Blood* **111**: 4297–4308.
- Yaron Y, McAdara JK, Lynch M, Hughes E, Gasson JC. (2001). Identification of novel functional regions important for the activity of HOXB7 in mammalian cells. *J Immunol* **166**: 5058–5067.
- Yatsula B, Lin S, Read AJ, Poholek A, Yates K, Yue D *et al.* (2005). Identification of binding sites of EVI1 in mammalian cells. *J Biol Chem* **280**: 30712–30722.
- Yuasa H, Oike Y, Iwama A, Nishikata I, Sugiyama D, Perkins A *et al.* (2005). Oncogenic transcription factor Evi1 regulates hematopoietic stem cell proliferation through GATA-2 expression. *EMBO J* **24**: 1976–1987.

Supplementary Information accompanies the paper on the Oncogene website (<http://www.nature.com/onc>)

Diagnostic utility of flow cytometry in low-grade myelodysplastic syndromes: a prospective validation study

Kiyoyuki Ogata,¹ Matteo G. Della Porta,² Luca Malcovati,² Cristina Picone,² Norio Yokose,³ Akira Matsuda,⁴ Taishi Yamashita,^{1,5} Hideto Tamura,¹ Junichi Tsukada,⁶ and Kazuo Dan¹

¹Division of Hematology, Department of Medicine, Nippon Medical School, Tokyo, Japan; ²Department of Hematology Oncology, University of Pavia Medical School and Fondazione IRCCS Policlinico San Matteo, Pavia, Italy; ³Division of Hematology, Department of Internal Medicine, Chiba Hokusoh Hospital, Nippon Medical School, Chiba, Japan; ⁴Department of Hematology, Saitama International Medical Center, Saitama Medical University, Saitama, Japan; ⁵Department of Industrial Science and Technology, Tokyo University of Science, Chiba, Japan, and ⁶First Department of Internal Medicine, School of Medicine, University of Occupational and Environmental Health, Fukuoka, Japan

ABSTRACT

Background

The diagnosis of myelodysplastic syndromes is not always straightforward when patients lack specific diagnostic markers, such as blast excess, karyotype abnormality, and ringed sideroblasts.

Design and Methods

We designed a flow cytometry protocol applicable in many laboratories and verified its diagnostic utility in patients without those diagnostic markers. The cardinal parameters, analyzable from one cell aliquot, were myeloblasts (%), B-cell progenitors (%), myeloblast CD45 expression, and channel number of side scatter where the maximum number of granulocytes occurs. The adjunctive parameters were CD11b, CD15, and CD56 expression (%) on myeloblasts. Marrow samples from 106 control patients with cytopenia and 134 low-grade myelodysplastic syndromes patients, including 81 lacking both ringed sideroblasts and cytogenetic aberrations, were prospectively analyzed in Japan and Italy.

Results

Data outside the predetermined reference range in 2 or more parameters (multiple abnormalities) were common in myelodysplastic syndromes patients. In those lacking ringed sideroblasts and cytogenetic aberrations, multiple abnormalities were observed in 8/26 Japanese (30.8%) and 37/55 Italians (67.3%) when the cardinal parameters alone were considered, and in 17/26 Japanese (65.4%) and 42/47 Italians (89.4%) when all parameters were taken into account. Multiple abnormalities were rare in controls. When data from all parameters were used, the diagnostic sensitivities were 65% and 89%, specificities were 98% and 90%, and likelihood ratios were 28.1 and 8.5 for the Japanese and Italian cohorts, respectively.

Conclusions

This protocol can be used in the diagnostic work-up of low-grade myelodysplastic syndromes patients who lack specific diagnostic markers, although further improvement in diagnostic power is desirable.

Key words: myelodysplastic syndromes, flow cytometry, diagnosis.

Citation: Ogata K, Della Porta MG, Malcovati L, Picone C, Yokose N, Matsuda A, Yamashita T, Tamura H, Tsukada J, and Dan K. Diagnostic utility of flow cytometry in low-grade myelodysplastic syndromes: a prospective validation study. *Haematologica* 2009;94:1066-1074. doi:10.3324/haematol.2009.008532

©2009 Ferrata Storti Foundation. This is an open-access paper.

Acknowledgments: we would like to thank all clinicians, technical staff, and patients of our institutions for their support of the work. We would further thank Kenji Takai, SRL, Inc. for his expertise on FCM and Mario Cazzola, University of Pavia Medical School and Fondazione IRCCS Policlinico San Matteo, Pavia for his thoughtful advice and support.

Funding: the Pavia investigations were supported by grants from the Associazione Italiana per la Ricerca sul Cancro (AIRC) and Fondazione IRCCS Policlinico San Matteo to Mario Cazzola.

Manuscript received on March 12, 2009. Revised version arrived on April 14, 2009. Manuscript accepted on April 15, 2009.

Correspondence: Kiyoyuki Ogata, Division of Hematology, Nippon Medical School, 1-1-5 Sendagi, Bunkyo-ku, Tokyo 113-8603, Japan. E-mail: ogata@nms.ac.jp

The online version of this article contains a supplementary appendix.